National Park Service
U.S. Department of the Interior

Natural Resource Stewardship and Science

Surface Water Area Change in the Arctic Network of National Parks, Alaska, 1985-2011

Analysis of Landsat Data

Natural Resource Data Series NPS/ARCN/NRDS—2013/445

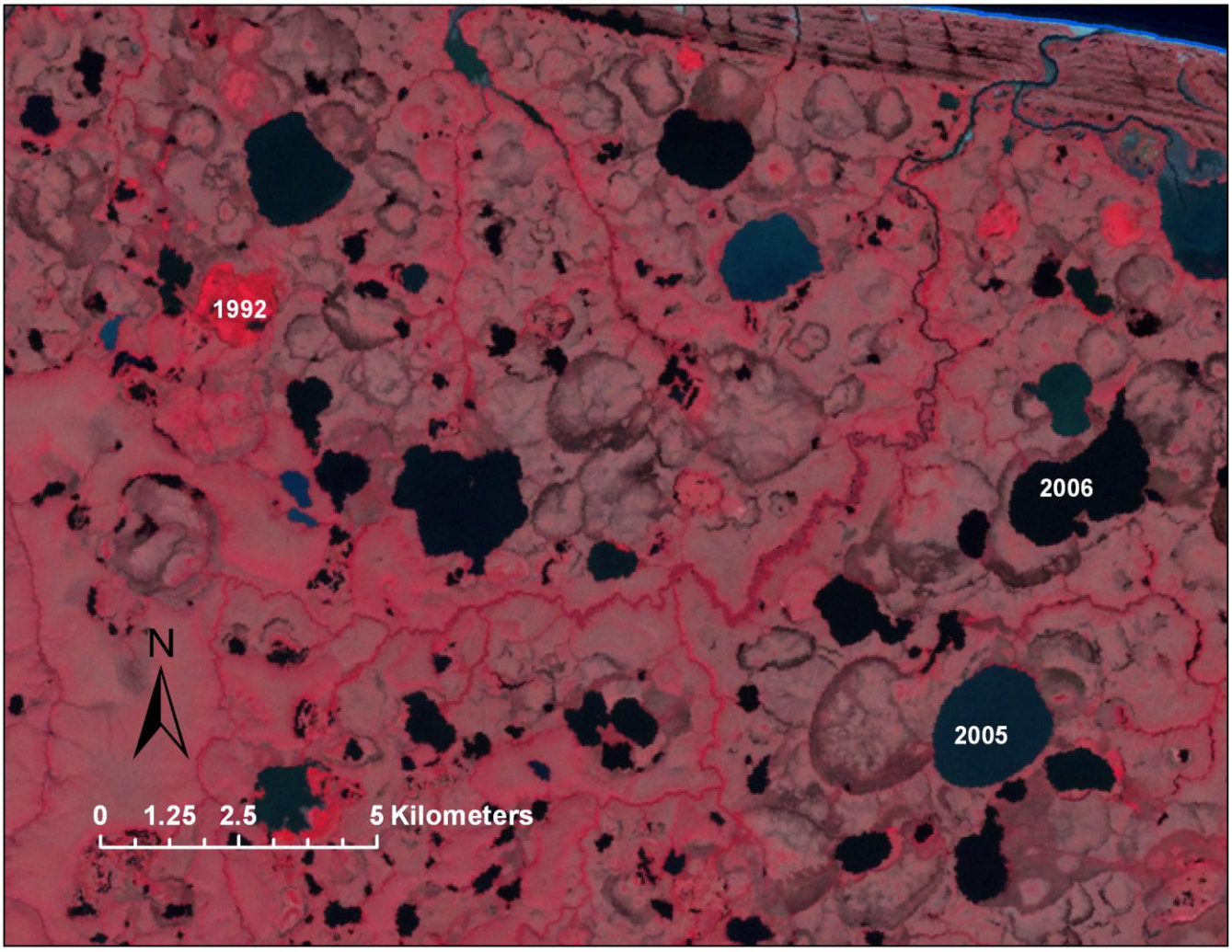

ON THE COVER

Landsat image of the Bering Straits Lower Coastal Plain in Bering Land Bridge National Preserve, Alaska, (color-infrared color scheme, 2002). The numerous lakes and ponds here occupy basins produced by thermokarst (subsidence from thaw of ice-rich permafrost). Roughly circular outlines of former lake basins that have drained are visible between existing lakes. The bright red basin labeled “1992” drained between 1992 and 1995; it is bright colored due to lush vegetation. The basins labeled “2005” and “2006” were last full in those years. Lake “2005” was nearly empty of water by 2006, while lake “2006” drained partially over the following two years.

Surface Water Area Change in the Arctic Network of National Parks, Alaska

Analysis of Landsat Data

Natural Resource Data Series NPS/ARCN/NRDS—2013/445

David K. Swanson

National Park Service
4175 Geist Road
Fairbanks, AK 99709

February 2013

U.S. Department of the Interior
National Park Service
Natural Resource Stewardship and Science
Fort Collins, Colorado

The National Park Service, Natural Resource Stewardship and Science office in Fort Collins, Colorado, publishes a range of reports that address natural resource topics. These reports are of interest and applicability to a broad audience in the National Park Service and others in natural resource management, including scientists, conservation and environmental constituencies, and the public.

The Natural Resource Data Series is intended for the timely release of basic data sets and data summaries. Care has been taken to assure accuracy of raw data values, but a thorough analysis and interpretation of the data has not been completed. Consequently, the initial analyses of data in this report are provisional and subject to change.

All manuscripts in the series receive the appropriate level of peer review to ensure that the information is scientifically credible, technically accurate, appropriately written for the intended audience, and designed and published in a professional manner.

This report received informal peer review by subject-matter experts who were not directly involved in the collection, analysis, or reporting of the data.

Views, statements, findings, conclusions, recommendations, and data in this report do not necessarily reflect views and policies of the National Park Service, U.S. Department of the Interior. Mention of trade names or commercial products does not constitute endorsement or recommendation for use by the U.S. Government.

This report is available from the National Park Service, Arctic Inventory and Monitoring Network (http://science.nature.nps.gov/im/units/arcn/) and the Natural Resource Publications Management website (http://www.nature.nps.gov/publications/nrpm/).

Please cite this publication as:

Swanson, D. K. 2013. Surface water area change in the Arctic Network of National Parks, Alaska, 1985-2011: analysis of Landsat data. Natural Resource Data Series NPS/ARCN/NRDS—2013/445. National Park Service, Fort Collins, Colorado.

NPS 953/119793, February 2013

Contents

Contents (continued)

Contents (continued)

Figures

Page

Figures (continued)

Page

Figures (continued)

Page

Figures (continued)

Page

Tables

Page

Abstract

The surface area of lakes and ponds was mapped across the National Park Service (NPS) Arctic Inventory and Monitoring Network (ARCN) using Landsat satellite images (30 m resolution) from 1985 to 2011. Trends in lake area were summarized for ecological subsections with greater than 1% cover by lakes and ponds. Many subsections had lake area increases that peaked around the year 2000, but lake area in all subsections was constant or declined after 2004. In subsections with constant lake area in the 2000s or slow rates of decrease (e.g., -0.4%/year), the area in 2010 was similar to what was present in the 1980s and 1990s. However, some subsections experienced major declines in surface water area in the 2000s, with rates of change of -1%/year to -3%/year and areas in 2010 that were 10% to 20% below what was present in the 1980s and 1990s. The subsections with the most substantial declines include: the Bering Straits Lower Coastal Plain (BSLCP) in Bering Land Bridge National Preserve; the Wulik Lowland in Cape Krusenstern National Monument; the Kobuk and Koyukuk River Valleys in Gates of the Arctic National Park and Preserve; the Nigeruk Plain in Kobuk Valley National Park; and the Noatak Glaciated Lowlands and the Upper Noatak Basin in the Noatak National Preserve. Subsections dominated by lakes of thermokarst origin (the BSLCP, Wulik Lowland, and Nigeruk Plain) lost lake area mainly by abrupt lake drainage events. In the other subsections showing declines in lake area, lakes were mostly in depressions on glacial deposits; here lake loss occurred by shrinkage of many lakes and ponds.

.

Acknowledgments

Thanks to Matt Macander of ABR Inc for helpful discussions and, with Chris Swingley of ABR, for creating the tiled Landsat image dataset used to create the ARCN composites. Thanks to Jon O'Donnell, Amy Larsen, and Jim Lawler of the NPS for helpful review comments.

Introduction

The lowlands of the NPS Arctic Inventory and Monitoring Network (ARCN, Fig. 1), like much of the arctic and subarctic, have extensive areas of lakes and ponds. According to the National Hydrography Dataset (USGS NHD 2012) there are approximately 1090 square kilometers of surface water in lakes and ponds in ARCN. The area of lakes and ponds in some parts of Alaska has declined in recent decades (Yoshikawa and Hinzman 2003, Riordan et al. 2006, Jones et al. 2011, Roach et al 2011). Whether these changes represent long-term trends, or are merely cycles that will eventually reverse, is an important question. Water bodies are of great interest, both as habitat for aquatic wildlife and as indicators of changes in the hydrologic balance. For this reason, ARCN has included monitoring of surface water area as a part of the Terrestrial Landscape Patterns and Dynamics Vital Sign (see the ARCN Terrestrial Landscape Patterns and Dynamics Vital Sign web site at http://science.nature.nps.gov/im/units/arcn/index.cfm?rq=12&vsid=28). Properties of lakes in ARCN are also monitored as a part of the Shallow Lakes Vital Sign (http://science.nature.nps.gov/im/units/arcn/index.cfm?rq=12&vsid=133) and the Lake Communities and Ecosystems Vital Sign (http://science.nature.nps.gov/im/units/arcn/index.cfm?rq=12&vsid=12). The purpose of the present study is to present data on surface water area available up to the present (year 2011) from Landsat satellite images, the source that will be used in the future to monitor surface water area as a part of the Terrestrial Landscape Patterns and Dynamics Vital Sign.

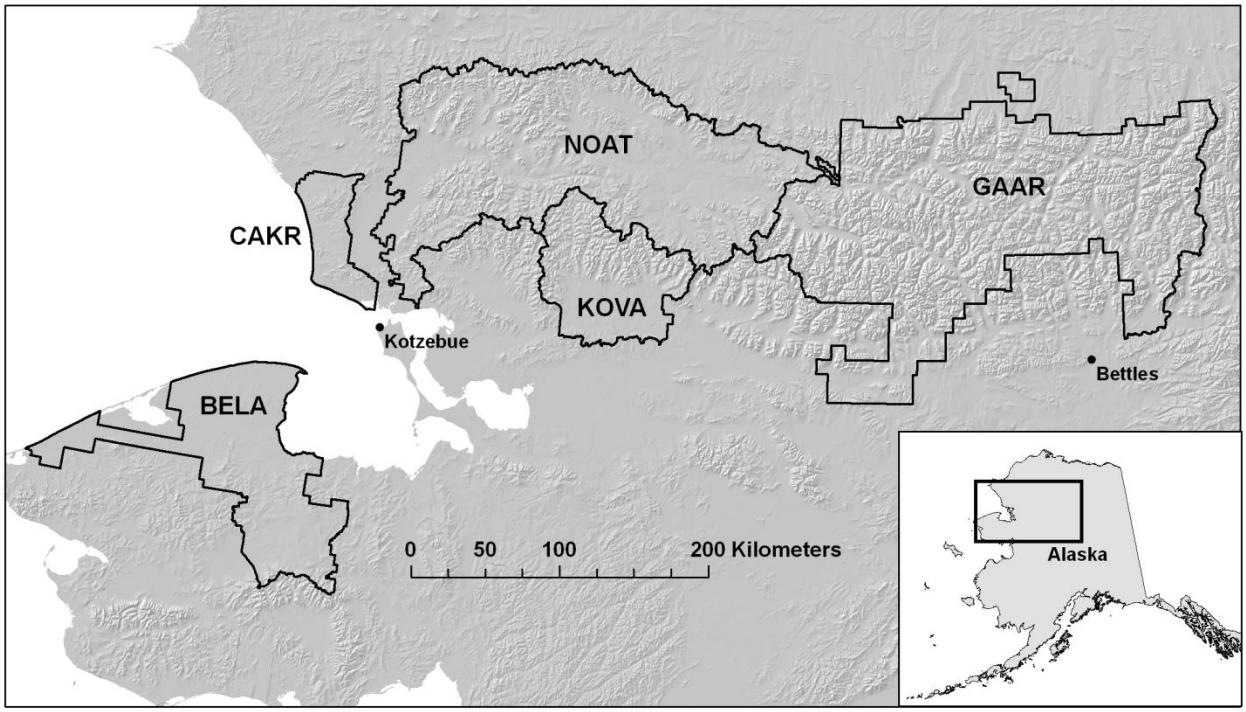

Figure 1. The NPS Arctic Inventory and Monitoring Network (ARCN). ARCN consists of 5 NPS units: Bering Land Bridge National Preserve (BELA), Cape Krusenstern National Monument (CAKR), Gates of the Arctic National Park and Preserve (GAAR), Kobuk Valley National Park (KOVA), and the Noatak National Preserve (NOAT).

Landsat images were chosen for a number of reasons. They are a readily available at no cost, they have a long record ranging back into the 1980s, and the Landsat program is expected to continue into the future (see http://www.nasa.gov/mission_pages/landsat/main/index.html). Landsat images have multiple wave bands, including the middle infrared (wavelength1.55-1.75 μm), which is especially useful for detection of surface water bodies. Finally, Landsat's moderate resolution (30 m pixels) is appropriate for an ARCN-wide investigation.

Study Area

Permafrost

Permafrost is ground that stays frozen for multiple years, with summer thaw affecting only a near-surface layer known as the active layer. Permafrost can contain ice in excess of what the pore space of the materials could hold as liquid water. If such sediments thaw, the water released flows away and the ground surface subsides, a process known as thermokarst (Czudek and Demek 1970). Thermokarst can both create water-filled depressions ("thaw" lakes and ponds; Hopkins 1949) and also channels through which water can drain out of depressions (Jorgenson and Osterkamp 2005). Water bodies absorb more summer heat than land areas, creating a positive feedback situation in ice-rich sediments where thaw causes subsidence and ponding of water, followed by additional thaw and more subsidence (Hopkins 1949, Plug and West 2009).

Most of ARCN lies within the continuous permafrost zone, which means that permafrost is present across 90% or more of the landscape (Jorgenson et al. 2008). Permafrost is discontinuous (permafrost present over 50% to 90% of the landscape) in the southern half of KOVA and the two southern lowland extensions of GAAR (Fig. 1); however, detailed maps of permafrost distribution are not currently available. There is no deep permafrost data (i.e., below a meter or so depth) available from anywhere in ARCN, and deep borehole data from the regional vicinity (Osterkamp 2007) is from land, not water bodies. Thus the status of permafrost under water bodies in ARCN is mostly unknown. We can infer with certainty that permafrost is absent beneath large lakes in the discontinuous permafrost zone (e.g., Walker Lake in GAAR) and present beneath small tundra ponds in continuous permafrost areas; but the state of permafrost in intermediate situations between these extremes is unknown.

Lake Origins

Glacial Lake Basins

Most of GAAR and NOAT were glaciated in the late Pleistocene (Hamilton 2010, 2011). In these areas most lakes occupy basins in glacial deposits created by glacial erosion or deposition. For example, most of the lakes in GAAR are in elongate troughs in glacial deposits, aligned with the axis of broad, U-shaped valleys sculpted by glaciers. Glaciers tend to exploit topographic lows created by tectonic forces, so at a larger scale, tectonics are also involved in creating these basins. Glacial lake basins would exist as topographic lows even in the absence of permafrost (unlike basins of purely thermokarst origin, as described below), though of course the presence of permafrost in the basin has profound effects on the hydrologic properties of a lakes (e.g., Kane and Hinzman 1989).

Older glaciations affected east-central CAKR and east-central KOVA (Karlstrom et al. 1964). On these older moraines, ground ice has accumulated to the point where thermokarst processes (see below) are also active in shaping the lake basins.

Basins in Eolian Sand Sheets

In the vicinity of the Great Kobuk Sand Dunes in KOVA are numerous lakes in basins that appear to be original depressions in a sand sheet (see the Ahnewetut Wetlands in the KOVA section of the Results). We infer this from field observations of sandy lake bottoms and exposures of sand in the topographically higher areas (c. 5 m higher) between the lakes. While permafrost is widespread on the inter-lake surfaces here, it is unlikely that these lakes are of

thermokarst origin, since there is probably not enough ground ice in the sand to account for the c. 5 m of relief. Similar non-thermokarst lake basins in sandy deposits are widespread on Alaska's North Slope (Jorgenson and Shur 2007).

Thermokarst Lake Basins

Lakes of thermokarst origin are common in parts of ARCN. Many of the lakes in BELA and KOVA (outside of the sand sheet area described above) are of thermokarst origin. Thermokarst lake basins owe their existence to the presence of large amounts of ground ice that has thawed locally to form a basin, surrounded by ground with the ice still intact (Hopkins 1949, Jorgenson and Shur 2007). The volume of ground ice limits the possible depth of a lake basin of purely thermokarst origin.

Much of the thermokarst lake terrain in ARCN has low relief of just a few meters. Here multiple overlapping lake basins of different ages are visible. Good examples are the Bering Straits Lower Coastal Plain (BELA) and the Lower Noatak Lowland (NOAT; see the Results section). This is the kind of terrain that gave rise to the notion of the "thaw-lake cycle" (Billings and Peterson 1980). By this model, lakes form by thermokarst and later drain by formation of an outlet channel, after which ice again accumulates in the sediments of the drained lake, raising the ground surface again and setting the stage for a new thermokarst basin to form. Because the relief in these landscapes is just a few meters; lakes are quite shallow. The multiple overlapping basins of different ages indicate shifting positions of the lakes over time.

In some parts of ARCN are fine-grained sediments known as "yedoma" which contain large amounts of ground ice (Kanevskiy et al 2011). Thermokarst basins in yedoma are often in excess of 10 m deep (West and Plug 2008, Shur et al. 2009; see The Bering Straits Upper Coastal Plain and Goodhope Bay Upper Coastal Plain in the BELA section of the Results). Much of the ice in yedoma is in very large ice wedges that formed during the Pleistocene when the climate was colder than today. Lake surface area in yedoma is less than in the flatter thermokarst plains discussed above, with extensive gentle slopes between the relatively deep lake basins.

Lakes of Volcanic Origin

In BELA are a set of nearly circular lake basins in volcanic materials: White Fish Lake, Devil Mountain Lakes, and Killeak lakes (all are in the Devil Uplands, see the BELA section of the Results). These lakes occupy maars, which are depressions formed by volcanic explosions (Beget et al. 1996). These maar basins are deeper and more stable than the numerous shallow thermokarst basins of plains that surround the Devil Uplands. A few other lakes in BELA are impounded in part by recent lava flow (Hopkins 1963).

Floodplain Lakes

There are numerous small lakes on river floodplains, in depressions marking former positions of river channels. These floodplain lakes are typically very close to active river channels and were removed from our analysis when the ecological subsections dominated by rivers were excluded (see Methods below).

Methods

The main steps in data analysis were to: 1) create cloud-free Landsat image composites, 2) classify the surface as water or land using Landsat band 5, 3) tabulate surface area by year and ecological subsection, 4) plot water area of each subsection vs. year and use regression analysis to detect trends.

Image Processing

Surface water area was mapped using Landsat satellite multispectral scanner data. The main data source was the middle infrared band (band 5, wavelength1.55-1.75 µm) of the Thematic Mapper (TM) sensor (NASA 2012) on Landsat 5 (1985-2011) and Landsat 7 (1999-2011). This band typically shows values of less than 250 for water and greater than 1000 for land. I used a threshold value of 600 to differentiate water (band 5 < 600) from land (band 5 ≥ 600). (These Landsat data values are unit-less reflectance - the proportion of incident light reflected - times 10,000; thus, for example, a value of 250 for band 5 in a particular pixel means that 2.5% of the solar energy in this wavelength range that struck the pixel was reflected.)

The challenge in using optical satellite imagery is cloud cover. A synthetic cloud-free image must be assembled from multiple images taken on different passes of the satellite, which are separated by 16 days. The result is known as a "composite" image and the process is termed "compositing". Two types of composites were used in this study: composites produced by the author (referred to as "ARCN" composites below) and composites produced by the U.S. Geological Survey as a part of its Web-enabled Landsat Data (WELD) Project (Roy et al. 2010 and http://landsat.usgs.gov/WELD.php).

WELD composites are available for 2003-2011. ARCN composites were computed for available years prior to 2003 and for a period of overlap with the WELD composites (2003-2005) to ensure that any differences between the two methods would not be interpreted as a change in lake area. The use of USGS WELD composites is a significant time savings over creating the composites locally.

ARCN Composites

The task in creating composites is to avoid pixels with clouds or cloud shadows. The latter are a particular problem because they have low values for all wave bands (including band 5) and thus could be confused with water. To create the ARCN composites I chose only pixels not labeled as "cloud" on the Landsat data deliverable (which eliminated most but not all cloudy pixels) and then tallied the number of image dates in a summer when each pixel contained a band 5 value less than 600 (which represent water, cloud shadow, or terrain shadow), or 600 or greater (which represent land or cloud). In water pixels the majority of images in a single summer have low band 5 values (with the occasional high value due to clouds), while in land pixels the majority of images from a single summer have high band 5 values (with an occasional low value due to cloud shadow).

The ARCN Landsat composites were assembled from a collection of images assembled by Matt Macander and Chris Swingley of ABR Inc. for another ARCN project (Macander and Swingley 2012). This collection contains all Landsat TM images available to date and judged visually to contain cloud-free areas. Macander and Swingley downloaded and preprocessed the images, and

divided them into co-registered 1000 by 1000 pixel tiles for ease in automated computations. The current study used only tiles that contained 50% or more cloud-free area. Preprocessing involved calibration of top-of-atmosphere reflectance and calculation of a cloud mask for each scene using the Landsat Ecosystem Disturbance Adaptive Processing System (LEDAPS, Masek 2006). For details see Macander and Swingley (2012).

ARCN composites were assembled from images taken in 1985, 1986, 1992, 1995, and 1999-2005. In the missing years between 1985 and 1999, Landsat 5 (the only functioning satellite at this time) did not return data for our area. Only images between June 20 and August 31 were used. This ensured that lakes would be ice-free and illuminated by a reasonably high sun angle.

To assemble the ARCN composites, a Python script was written for ArcMap GIS software that performed the following sequence of operations for each pixel: search all images in the year (between June 20 and August 31) for pixels not labeled in the original data as "cloud", if the pixel has a band 5 value < 600, tally 1 count for that pixel on a "dark" output raster for that tile; if the pixel has a band 5 value ≥ 600, tally 1 count for that pixel on a "light" output raster for the tile. After all the available images for a single year's summer have been search and tallied, compare the "dark" and "light" counts for each pixel: if 50% or more of the total cloud-free counts were "dark", label the pixel as water, otherwise, label it as land. This computational method returns a result similar to a median operation, without the considerable computer processing time that would be required to compute many medians from data strings of different lengths.

By this method both water bodies and areas under consistent terrain shadow (north sides of mountains) were labeled as "water". The shadow areas were eliminated in a step (described further below) where ecological subsections were used to extract the relatively flat lowlands where nearly all of ARCN's lakes occur.

In practice there were not enough images each summer to allow production of a cloud-free ARCN-wide composite. Thus I aggregated multiple years of data, by simply summing the "dark" and "light" counts from multiple years before finding the majority. The "1985" data point is actually 1985 and 1986, "1995" is actually 1992, 1995, and 1999, and the remaining years are 3 consecutive years assigned to the middle year: "2000" is 1999 through 2001, "2001" is 2000 through 2002, etc. These aggregations of 2 or 3 years provided enough images to have cloud-free values for nearly every pixel.

WELD Composites

The WELD program has produced summer (June, July, and August) composites of each year since 2003 as co-registered 5000 by 5000 pixel tiles across all of the United States. The algorithm used to detect cloudy pixels is described in Roy et al. (2011). These images have also been reflectance calibrated as described in Roy et al. (2011). As in the case of the ARCN composites, single-year composites – even if they include an entire summer – fail to completely cover ARCN with cloud-free data. The cloudiness problem is aggravated in WELD data by the fact that since 2003 the satellite it is based on (Landsat 7) has had a malfunction that causes it to omit strips of data, which must be filled from other dates. So again I aggregated 3 years of data, in this case by computing the median of band 5 for each pixel from 3 consecutive years and assigning the value to the middle year. Thus from the available data (years 2003 through 2011), I

was able to calculate 3-year running medians that could be assigned to years 2004 through 2010. This computation produced some smoothing of year-to-year variation, which is acceptable here because we are interested in long-term trends.

The resulting 3-year composites of Landsat band 5 were classified as water or land by the same criterion used previously: “water” for band 5 values less than 600, “land” for band 5 values of 600 or more.

Summary of Trends

Lake area was summed for each year by ecological subsection (Boggs and Michaelson 2001, Jorgenson 2001, Jorgenson et al. 2001, Swanson 2001a, 2001b). Subsections are areas of land with a relatively uniform climate and a consistent pattern of landforms, soils, and vegetation. Subsections help us to partition the variability in lake surface area across the landscape, because lakes within a subsection have similar hydrologic conditions. In addition, subsections provided a way to avoid various non-target areas: 1) salt water bodies (lagoons), 2) large floodplains (e.g. the Noatak River), where most of the water is in rivers and subject to large year-to-year variations associated with the timing of the images used in the composite; and 3) mountainous areas, where there are very few lakes but extensive terrain shadows that are difficult to differentiate from water on Landsat images. Thus I analyzed the lake area trends for all lowland subsections with at least 1% cover by surface water bodies, excluding those where surface water was dominantly rivers or salt water.

Subsections in GAAR were less useful for summarizing lake trends, because they combine lake-rich lowlands with uplands that have terrain shadow problems and no lakes. Thus, in GAAR I created analysis regions that covered the lake-rich parts of each major river valley: Alatna, Itkillik, Killik, Kobuk, Koyukuk, Nigu, and Noatak. The Anaktuvuk, Chandler, and John River valleys were not analyzed because within the GAAR perimeter most of the lakes in these valleys are on private land. Although the analysis regions were named after major rivers, they were drawn to avoid actual river floodplains for the same reasons that river-dominated subsections were excluded (see above).

Linear least-squares regressions of summed water area (in each subsection) vs. year were computed. Regressions were computed for the 6 consecutive years of water area based on the ARCN composite images (2000-2005) and separately for the 7 consecutive years of water area based on WELD composite images (2004-2010; the entire length of record). The significance of the regression slopes was evaluated by t-test. The ARCN and WELD data sets were not pooled for regression analysis, to avoid possible false trends due to differences in the two compositing methods.

Plots of water area vs. year for each subsection were compared to the classified images to help understand the source of any changes. This process revealed a few cloud errors on the classified images. These data points were removed and regressions repeated. The specific subsections, composites, and years of omitted data are as follows: BSLCP WELD 2007 (in BELA); and Kobuk ARCN 2000-2001, Koyukuk ARCN 2004, and Nigu WELD 2010 (in GAAR). The yearly images were also examined for lakes that substantially drained or filled between years. The identification codes and areas for these lakes were recorded from the National Hydrography

Dataset (USGS NHD 2012). No formal minimum lake area was established for this process, but I consider the list of drained lakes to be comprehensive for lakes larger than 0.1 km^2 (10 ha).

Results

Data Presentation

Regressions of lake area vs. year for the two study data sets (2000-2005 ARCN Landsat composites and 2004-2010 WELD Landsat composites) are summarized by subsection in Table 1. Lake area change results are presented below by NPS unit and subsection. Under each subsection heading is a location map (Fig. 2 and following) and a plot of lake area vs. year (Fig. 3 and following). In Fig. 3 and the following graphs, triangles represent areas computed from ARCN Landsat composites (2000-2005) and circles represent areas computed from WELD Landsat composites (2004-2010). Trendlines and correlation coefficients (R^2) are shown on the graphs for all regressions where the t-test probability of zero slope was 0.1 or smaller. A table of all lake drainage or filling events noted in this study is in the Appendix.

Overview of Results

The results for each subsection are unique, but several patterns are apparent. 1) Many subsections had lake area increases that peaked around the year 2000, but lake area in all subsections was stable or declined since 2004. 2) The recent declines have ranged from minor in some areas (e.g., rates of change of -0.4%/year or less, and final areas similar to what was present in the 1980s and 1990s) to major in others (rates of change in excess of -1%/year and final areas 10% to 20% below what was present in the 1980s and 1990s). Subsections with these more substantial declines include: the Bering Straits Lower Coastal Plain (BSLCP) in BELA; the Wulik Lowland in CAKR; the Kobuk and Koyukuk River Valleys in GAAR; the Nigeruk Plain in KOVA; and the Noatak Glaciated Lowlands and the Upper Noatak Basin in NOAT. The lakes of the BSLCP, Wulik Lowland, and Nigeruk Plain are mostly of thermokarst origin, while lakes in the remaining subsections with significant declines are mostly in depressions on glacial deposits with minor thermokarst effects.

Table 1. ARCN lake change summary: regressions of lake area vs. year for 2000 to 2010 by ecological subsection

NPS Unit	Subsection Code	Subsection Name	Subsection Area, km^2	Lake Area, km^2	Regression years 2000-2005[1]			Regression years 2004-2010[2]		
					Slope, %/year[3]	R^2	t-test *P*	Slope, %/year[3]	R^2	t-test *P*
BELA	BSLCP	Bering Straits Lower Coastal Plain	1640	151	-0.75	0.59	0.074	**-1.19**	0.69	0.040
BELA	BSUCP	Bering Straits Upper Coastal Plain	1329	83	-0.31	0.54	0.098	**-0.47**	0.73	0.015
BELA	DU	Devil Uplands	826	81	**-0.32**	0.72	0.032	-0.02	0.01	0.826
BELA	GBLCP	Goodhope Bay Lower Coastal Plain	117	7	-0.25	0.43	0.160	0.26	0.3	0.207
BELA	GBUCP	Goodhope Bay Upper Coastal Plain	1322	40	-0.35	0.25	0.310	0.02	0	0.951
BELA	IL	Imuruk Lowlands	339	79	-0.24	0.47	0.134	-0.14	0.34	0.168
BELA	KZL	Kuzutrin Lowlands	226	10	**0.92**	0.78	0.020	-0.44	0.43	0.112
CAKR	ACP	Aukulak Coastal Plain	114	3	-1.31	0.50	0.114	**-1.81**	0.70	0.018
CAKR	IMP	Imikruk Plains	18	2	-0.15	0.05	0.684	0.09	0.01	0.819
CAKR	KOP	Kotlik Coastal Plain	146	4	**0.65**	0.68	0.044	0.01	0	0.978
CAKR	LNM	Lower Noatak Moraine	97	4	-0.19	0.13	0.481	**-0.72**	0.67	0.025
CAKR	WUL	Wulik Lowland	375	3	-1.49	0.62	0.065	**-1.52**	0.72	0.016
GAAR	Alatna	Alatna River Valley	35	5	-0.43	0.15	0.453	**-0.60**	0.72	0.016
GAAR	Itkillik	Itkillik River Valley	30	5	-0.06	0.03	0.741	**-0.20**	0.57	0.051
GAAR	Killik	Killik River Valley	103	5	-0.25	0.43	0.156	**-0.56**	0.69	0.020
GAAR	Kobuk	Kobuk River Valley	249	3	-1.16	0.48	0.307	**-1.41**	0.77	0.009
GAAR	Koyukuk	Koyukuk River Valley	250	5	**-0.90**	0.87	0.020	**-2.85**	0.93	<0.001
GAAR	Nigu	Nigu River Valley	85	3	-0.43	0.40	0.180	**-0.89**	0.78	0.020
GAAR	Noatak	Noatak River Valley	179	11	0.23	0.42	0.165	**-0.56**	0.84	0.003
KOVA	AHW	Ahnewetut Wetlands	154	17	-0.34	0.28	0.285	-0.69	0.40	0.126
KOVA	AKP	Akillik Plain	384	6	**3.16**	0.90	0.004	**-3.76**	0.90	0.001
KOVA	NIP	Nigeruk Plain	761	10	-0.92	0.19	0.385	**-3.06**	0.82	0.005
NOAT	AGU	Avingyak Glaciated Uplands	231	27	-0.10	0.16	0.435	**-0.37**	0.90	0.001
NOAT	IGU	Iggiruk Uplands	1006	31	-0.43	0.47	0.135	**-0.96**	0.87	0.002
NOAT	KGU	Kavachurak Glaciated Uplands	588	17	**-1.15**	0.75	0.025	**-0.76**	0.92	0.001
NOAT	LNL	Lower Noatak Lowlands	404	41	0.02	<0.01	0.952	-0.12	0.04	0.666
NOAT	MNU	Middle Noatak Uplands	558	24	0.00	<0.01	0.994	**-0.38**	0.75	0.012
NOAT	NGL	Noatak Glaciated Lowlands	727	30	**-1.31**	0.83	0.012	**-1.21**	0.89	0.001
NOAT	NGU	Nigu Mountain Valley	222	8	-0.54	0.46	0.137	**-0.79**	0.68	0.023
NOAT	UNB	Upper Noatak Basin	2626	54	**-0.88**	0.65	0.052	**-1.62**	0.91	0.001

[1]Linear least-squares regression for lake area in 6 years (2000-2005), lake area data from Landsat data composites by ARCN

[2]Linear least-squares regression for lake area in 7 years (2004-2010), lake area data from Landsat data composites by USGS WELD

[3]Regression slope is expressed as change in lake area per year as a percent of the 2004-2010 average cover (**boldface** where P ≤ 0,05).

Bering Land Bridge National Preserve

Lake area declined after 2000 in most subsections in BELA, but in most cases the declines were not statistically significant and came after relatively high levels in the early 2000s; as a result, lake areas in the late 2000s were still within the range of what was observed in the 1980s and 1990s. In one subsection, the Bering Straits Lower Coastal Plain, the lake area declined more rapidly after 2000 by multiple major lake drainage events, and the final area was well below what was present in the 1990s. This subsection has the most dynamic lakes in BELA, with numerous shallow thermokarst lakes prone to rapid draining, occasional refilling, and expansion by thermokarst

Bering Straits Lower Coastal Plain (BSLCP)

This subsection is the largest area of typical arctic thaw lakes in the study area. Lakes are dominantly of thermokarst origin, and multiple overlapping lake basins have formed by thaw subsidence/lake formation, lake drainage, re-formation of permafrost and ground ice, and new thaw subsidence/lake formation (Fig. 4). Part of this subsection lacks 1985-86 imagery, hence the missing 1985 data point in Fig. 3. The regression for lake area vs. year for 2000-2005 has a moderate slope (-0.70%/year) that is marginally significant with P = 0.07. For 2004-2010 the regression is highly significant and the slope steeper (-1.19%/year; Table 1, Fig. 3). (The low point in 2007 was due to a cloud error, and this point was omitted from the regression analysis.) Total lake area dropped most between 2003 and 2006, about 14 km^2 or 8.5%. Multiple large lake drainage events have been recorded in this subsection, and several around 2005 can account for about 10 km^2 of the drop in lake area near this time (Appendix). This subsection covers most of the study area of Jones et al. (2011). Their analysis was based on aerial photographs from 1950-51 and 1978 and high-resolution satellite imagery from 2006-07. Their longer-term data set revealed a 26% decline in area of lakes larger than 40 ha, with the entire decline occurring between 1978 and 2006-07.

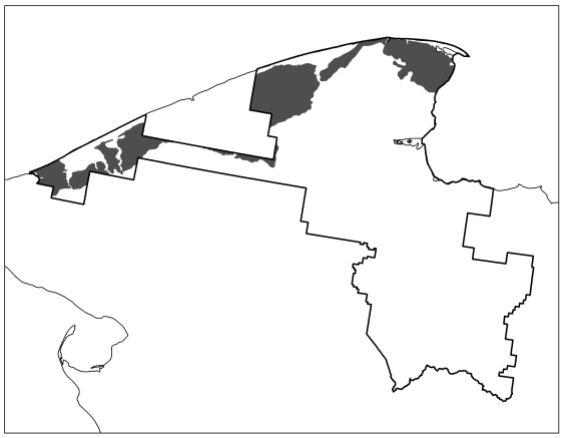

Figure 2. Location of the Bering Straits Lower Coastal Plain subsection in BELA

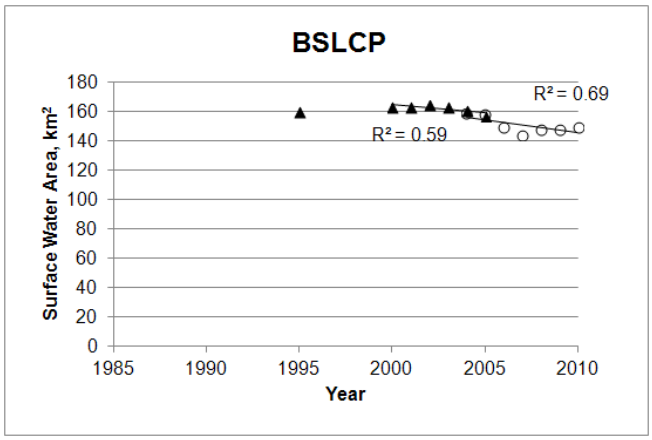

Figure 3. Plot of total surface water area vs. year for the Bering Straits Lower Coastal Plain subsection. Here and in all subsequent graphs, triangles represent areas computed from Landsat composites created by ARCN; circles represent areas computed from WELD Landsat composites. Trendlines and correlation coefficients (R^2) are shown for all regressions where P < 0.1. The 2007 point was low due to cloud error and omitted from the analysis.

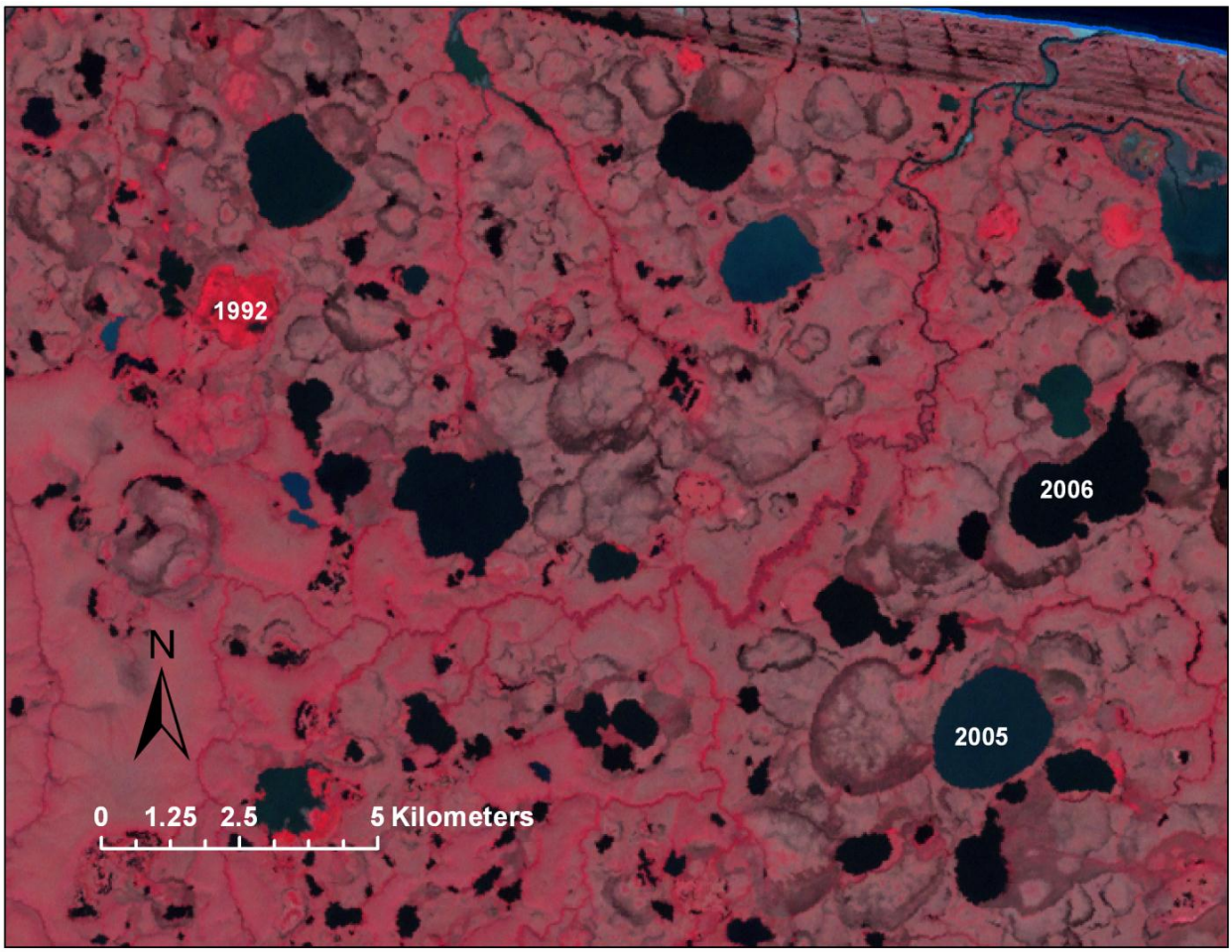

Figure 4. Bering Straits Lower Coastal Plain, Landsat image, color-infrared color scheme, 2002. The numerous lakes and ponds here occupy basins produced by thermokarst (thaw and subsidence of ice-rich permafrost). Roughly circular outlines of former lake basins that have drained are visible between existing lakes, and overlapping basins are common. The bright red basin labeled “1992” drained between images taken in 1992 and 1995 and is bright colored due to lush vegetation. The basins labeled 2005 and 2006 were last full in those years. Lake “2005” was nearly empty of water by 2006, while lake “2006” drained partially over the next two years.

Bering Straits Upper Coastal Plain (BSUCP)

This subsection contains lakes of mainly thermokarst origin, in deep basins in ice-rich Pleistocene "yedoma" sediments (Fig. 7). Part of this subsection lacks 1985-86 imagery. Lake area increased 1995-2000, mainly by increase in the areas of smaller lakes, the largest of which are listed in the Appendix. Lake area appears to have declined since 2004 (with a highly significant regression for years 2004-2010), though the rate of decline was modest and the area had yet to decline to its 1995 level. Only one major drainage event was observed (Appendix).

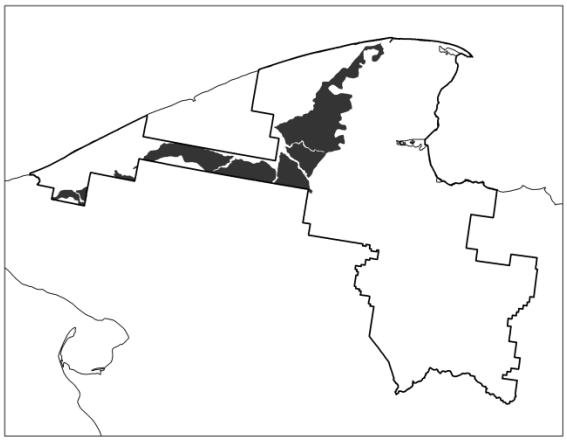

Figure 5. Location of the Bering Straits Upper Coastal Plain subsection in BELA

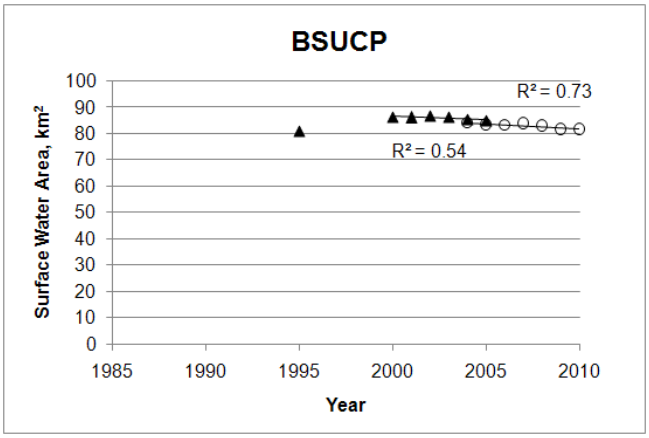

Figure 6. Plot of total surface water area vs. year for the Bering Straits Upper Coastal Plain subsection.

Figure 7. "Yedoma" lake landscape in BELA. Very ice-rich silty "yedoma" deposits dominate the Bering Straits Upper Coastal Plain subsection. Lakes are of mainly thermokarst origin and are in deep basins due to thaw of large amounts of ice. (August 2010 photo.)

Devil Uplands (DU)

This subsection is dominated by large, stable maar lakes, though it also contains some smaller lakes that could be of thermokarst origin in yedoma-like sediments. Lake area has varied little relative to the large total area thanks to the generally large, deep and stable lake basins. There was an apparent drop of about 2 km^2 area (2%) from 1985 to 1995, largely due to the drainage of two basins (Appendix). The area recovered this lost area by 2000 (though not by refilling of these basins) and then declined (with significant regression for 2000-2005), though the rate of decline was modest and subsequently leveled off.

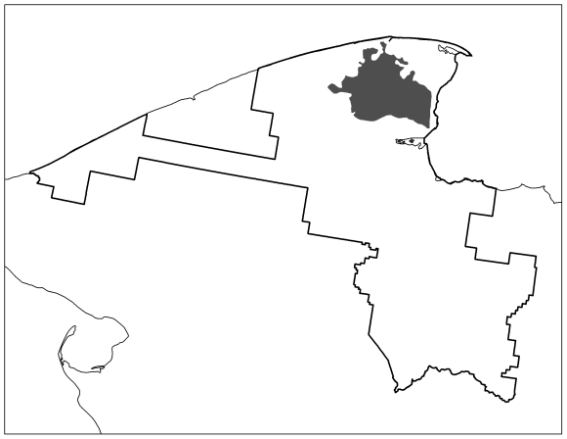

Figure 8. Location of the Devil Uplands subsection in BELA

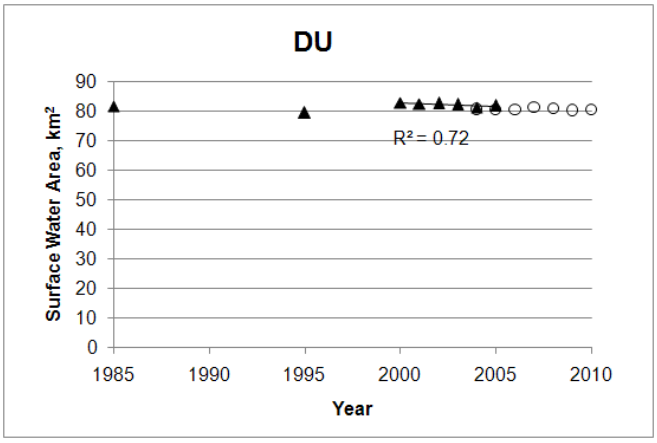

Figure 9. Plot of total surface water area vs. year for the Devil Uplands subsection.

Goodhope Bay Lower Coastal Plain (GBLCP)

This is another low plain dominated by cyclical thaw lakes. Lake area has been quite constant except for 1995, when it was about 10% lower than the rest of the observation period, primarily due to some drainage events between 1985 and 1992. Lake area then recovered by partial refilling of some basins and expansion of others.

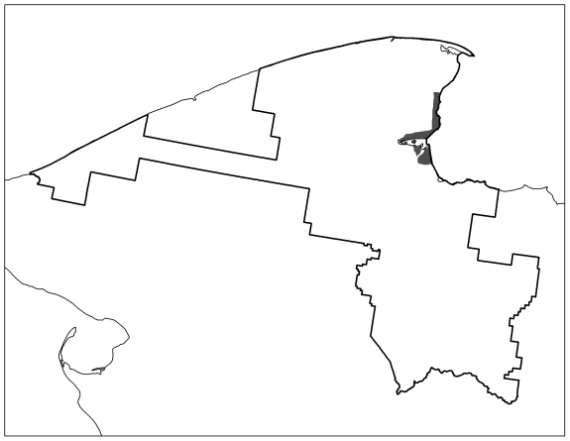

Figure 10. Location of the Goodhope Bay Lower Coastal Plain subsection in BELA

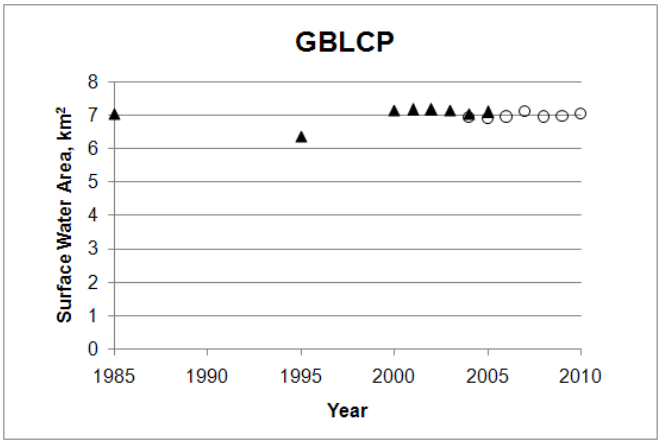

Figure 11. Plot of total surface water area vs. year for the Goodhope Bay Lower Coastal Plain subsection.

Goodhope Bay Upper Coastal Plain (GBUCP)

This is another area of deep thermokarst lake basins in ice-rich yedoma sediments. Lake area increased by about 3 km^2 (8%) from 1985 to 2000 by widespread expansion along lake and pond edges. This occurred in spite of a minor drainage event (Appendix). Some minor lake shrinkage has occurred since, but not enough to produce significant regressions of lake area vs. year.

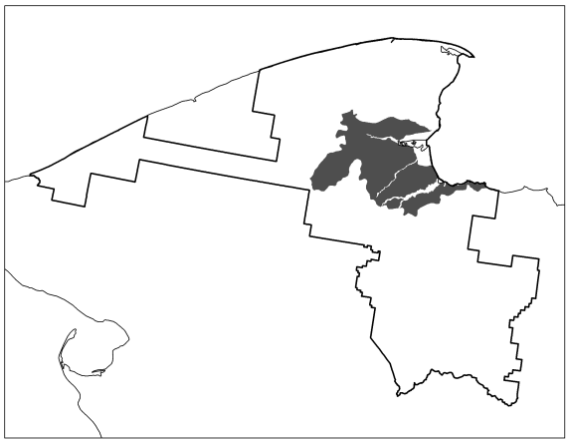

Figure 12. Location of the Goodhope Bay Upper Coastal Plain subsection in BELA

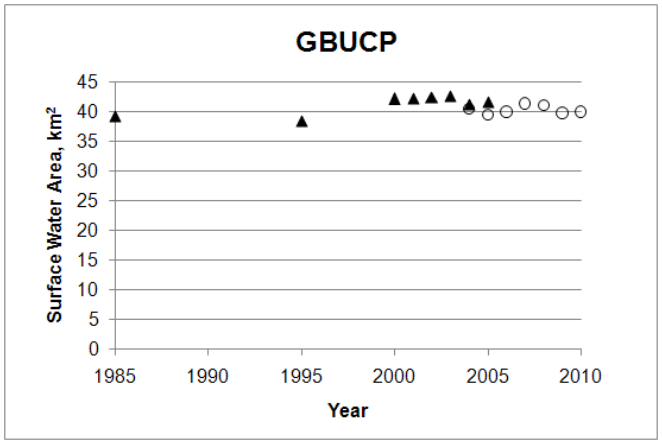

Figure 13. Plot of total surface water area vs. year for the Goodhope Bay Upper Coastal Plain subsection.

Figure 14. Lake in the Goodhope Bay Upper Coastal Plain. Very ice-rich silty "yedoma" deposits dominate this subsection. Lakes are of mainly thermokarst origin and are in deep basins due to thaw of large amounts of ice. Hummocks on the steep far bank of the lake are remnants of ice wedge polygon centers. (August 2010 photo.)

Imuruk Lowlands (IL)

Despite multiple small thermokarst lake drainage events through the 2000s, this small subsection did not display a significant change in lake area, probably because the trend was dominated by the large and stable Imuruk Lake

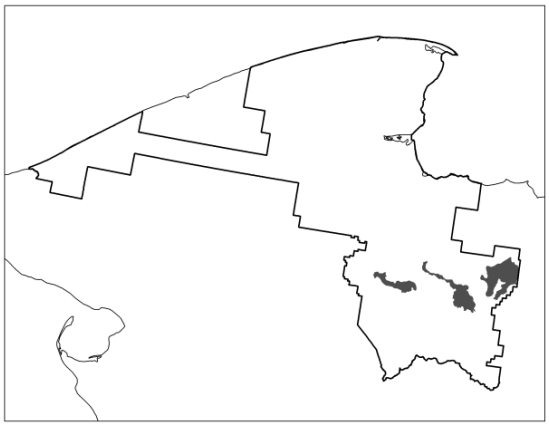

Figure 15. Location of the Imuruk Lowlands subsection in BELA

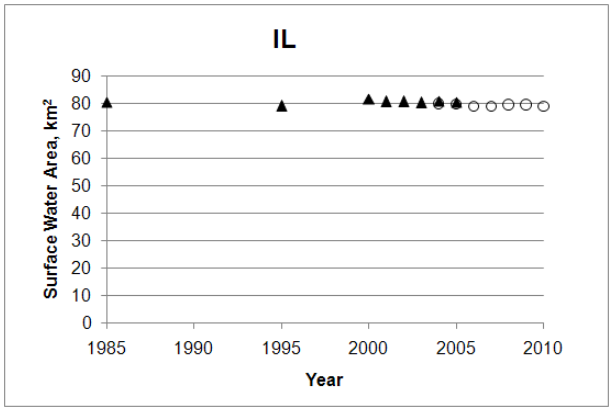

Figure 16. Plot of total surface water area vs. year for the Imuruk Lowlands subsection.

Kuzutrin Lowlands (KZL)

This small subsection with thermokarst depressions has experienced multiple minor fluctuations in lake area. The 2000-2005 regression showed a significant increase, though this appears to have only brought lake area back to 1985 levels and subsequent trends have been weak.

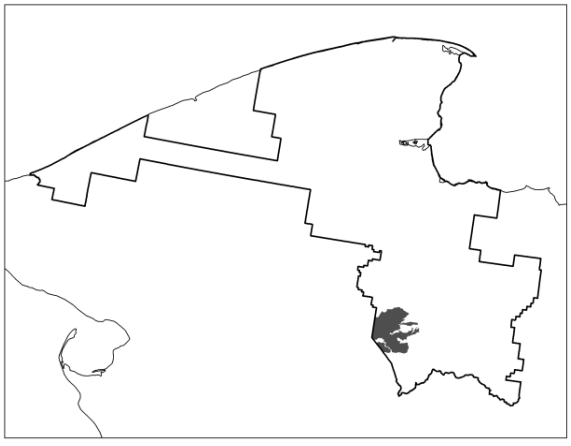

Figure 17. Location of the Kuzitrin Lowlands subsection in BELA

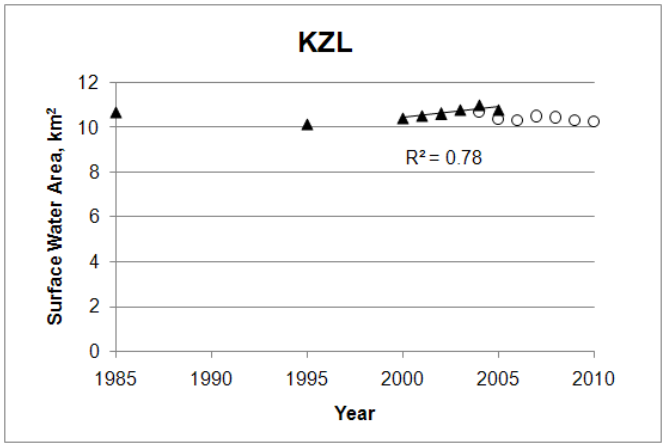

Figure 18. Plot of total surface water area vs. year for the Kuzitrin Lowlands subsection.

Cape Krusenstern National Monument

Trends in lake area differed between subsections in CAKR, due in some cases to events at a few large lakes. Lake area since 2004 was stable or declining in all subsections, though in two of the three subsections with declines the rate of decline was gradual (LNM) or lake area merely declined to pre-2000 levels after a high in the early 2000s (ACP). The Wulik Lowlands subsection experienced a more serious decline, dropping about 16% since 2000.

Aukulak Coastal Plain (ACP)

This subsection has multiple small lakes of probable thermokarst origin; it is mostly integrated by a drainage network and is only partly covered by present and former lake basins. Lake area increased by more than 0.5 km^2 (almost 20%), between 1995 and 2000 (Fig. 20), by expansion of many lakes, in spite of the loss of one small lake during this time (Appendix). Subsequent declines, as evidenced by highly significant regression for 2004-2010, have brought the area back down to its pre-2000 level.

Figure 19. Location of the Aukulak Coastal Plain subsection in CAKR

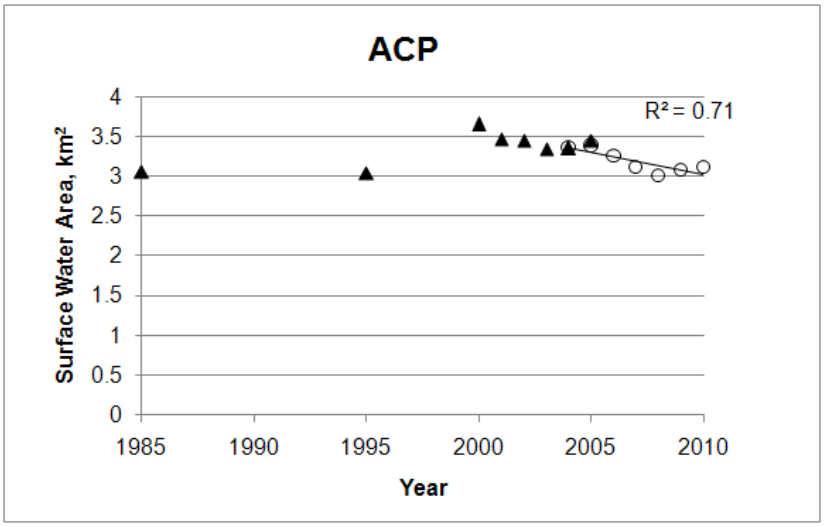

Figure 20. Plot of total surface water area vs. year for the Aukulak Coastal Plain subsection.

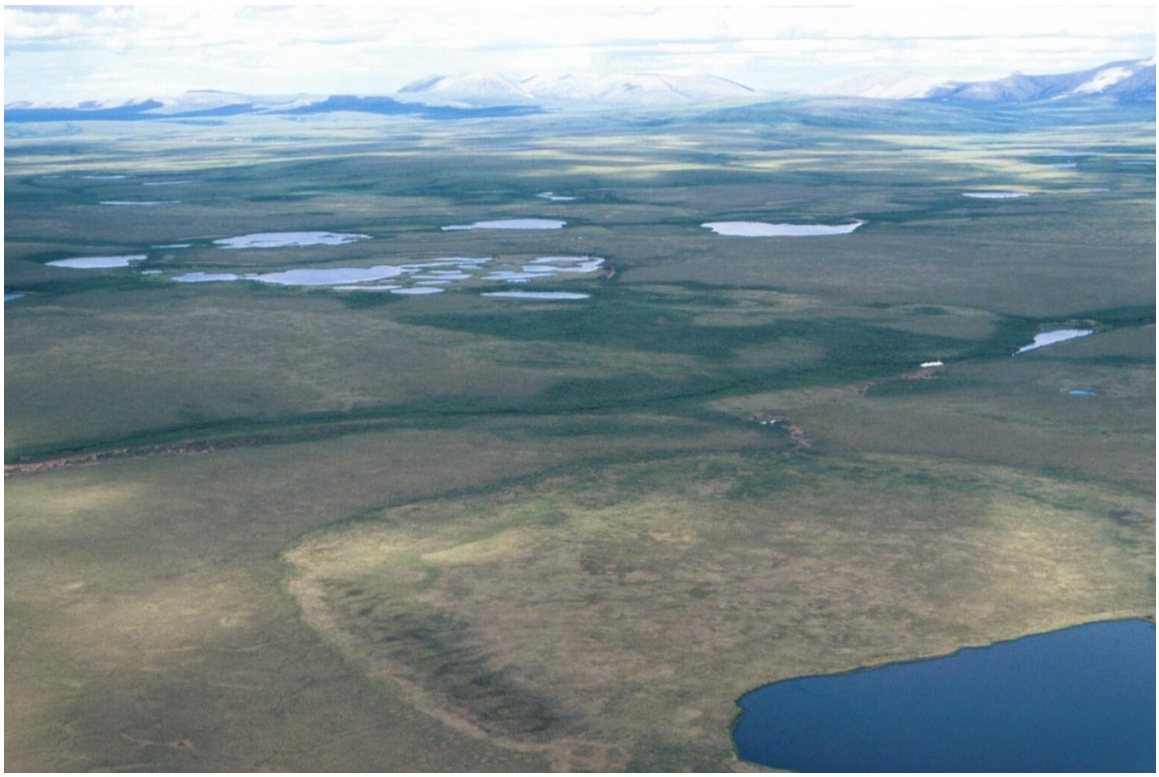

Figure 21. Aukulak Coastal Plain lakes. These lakes are mainly of thermokarst origin. The lake in the right and center foreground drained prior to 1985 by formation of a channel linking to the drainageway that runs from right to left across the middle of the photograph. (July 2001 photo.)

Imikruk Plain (IMP)

This extensive coastal plain with many overlapping thermokarst basins lies mostly outside of the NPS unit boundaries. The portion in CAKR has shown weak trends during our study period, though areas in the 2000s appear higher than in 1995. Data are missing from 1985.

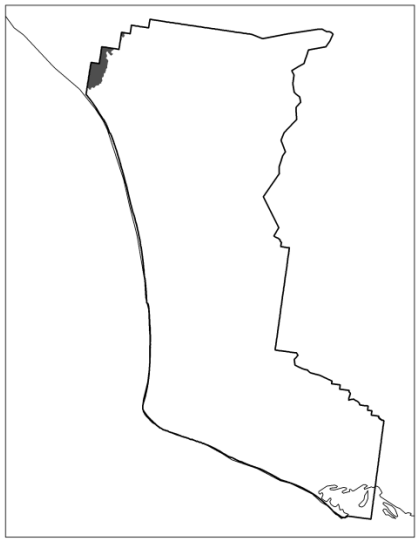

Figure 22. Location of the Imuruk Plain subsection in CAKR

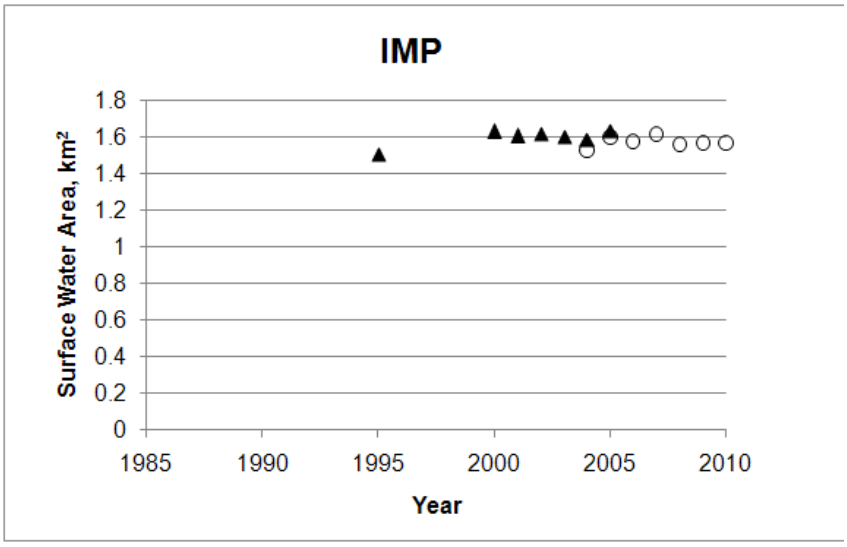

Figure 23. Plot of total surface water area vs. year for the Imuruk Plain subsection.

Kotlik Coastal Plain (KOP)

This subsection resembles the Aukulak Coastal Plain, with multiple small lakes of probable thermokarst origin. Lake area appears to have dropped 1985 to 1995, increased through 2005, and then stabilized thereafter near 1985 levels.

Figure 24. Location of the Kotlik Coastal Plain subsection in CAKR

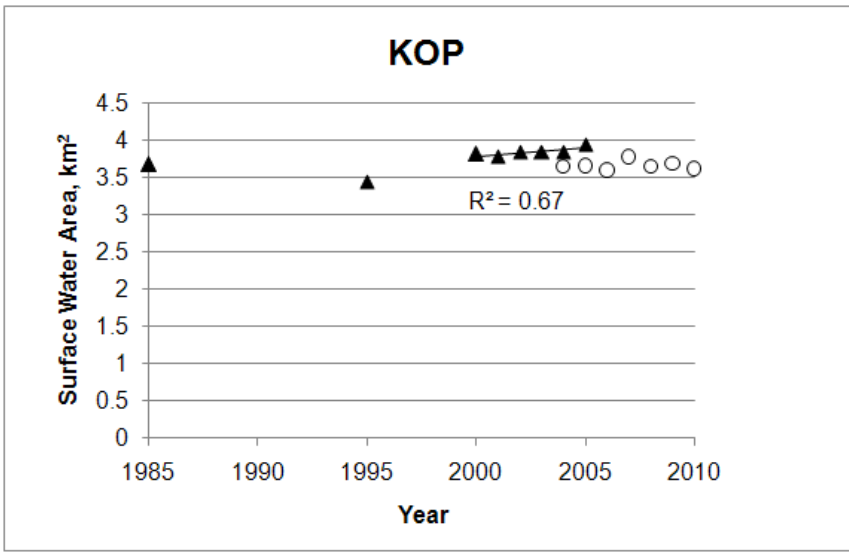

Figure 25. Plot of total surface water area vs. year for the Kotlik Coastal Plain subsection.

Lower Noatak Moraine (LNM)

This is an area of low-relief glacial moraine. Lake basins are depressions in the moraine surface that have been modified by thermokarst. Lake area dropped by 0.75 km^2 (15%) from 1985 to 1995, mainly due to the partial drainage of one relatively large lake (Fig. 28, Appendix). Lake area stabilized for a time, then resumed its decline by the shrinkage of multiple lakes; the period 2004-2010 had a statistically significant decline, though the slope was fairly gentle (-0.7%.year).

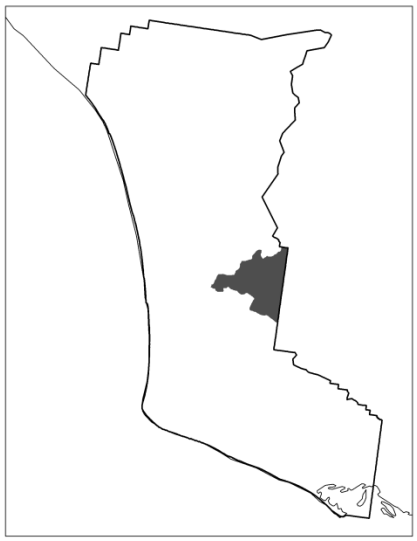

Figure 26. Location of the Lower Noatak Moraine subsection in CAKR

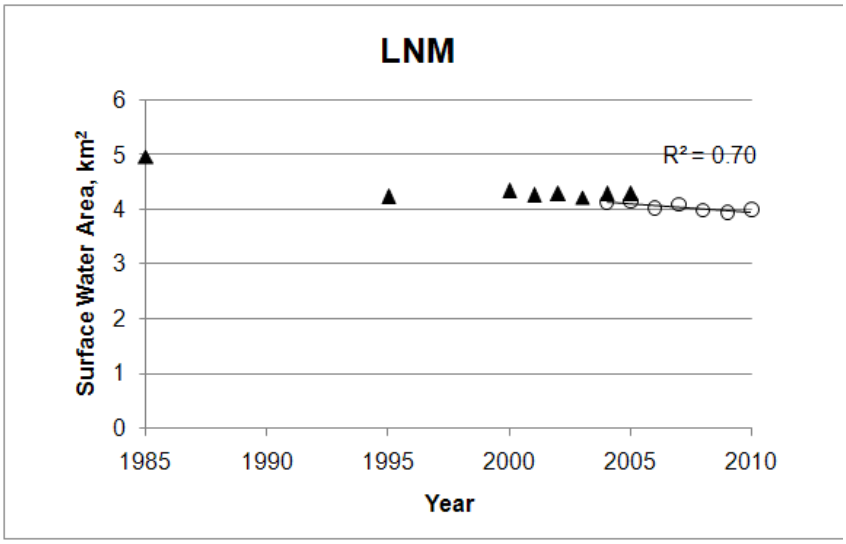

Figure 27. Plot of total surface water area vs. year for the Lower Noatak Moraine subsection.

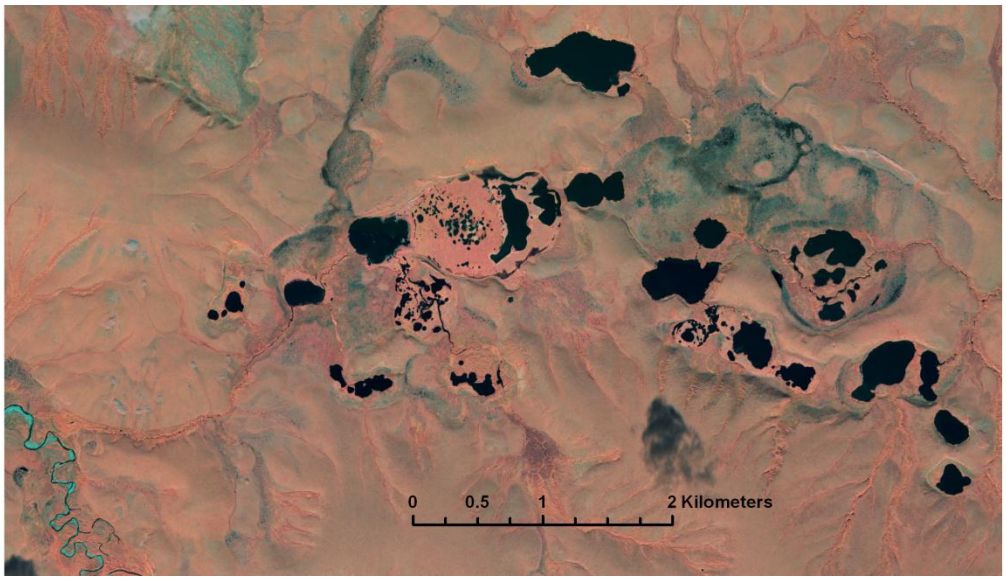

Figure 28. Lake drainage in the Lower Noatak Moraine subsection. The complex of lakes in the right half of the photograph partly drained prior to 1985 by channels leading to the right. The large oval basin near the center of the photo drained over half way between 1985 and 1992 by a channel leading to the left into the Kilikmak Creek. The bright reddish colors in this basin result from vigorous green vegetation growing on the former lake bottom. (IKONOS satellite image, color-infrared color scheme, August 2006.)

Wulik Lowland (WUL)

This is an extensive plain in northern CAKR with relatively few lakes and a generally integrated drainage network. Lake area appears to have been mostly stable prior to 2000 and then declined to about 16% below the 1985-2000 level. The decline since 2005 was statistically significant at about -1.5% per year. The decline was due to two major drainage events (Fig. 31, Appendix) and less drastic shrinking of other lakes.

Figure 29. Location of the Wulik Lowland subsection in CAKR

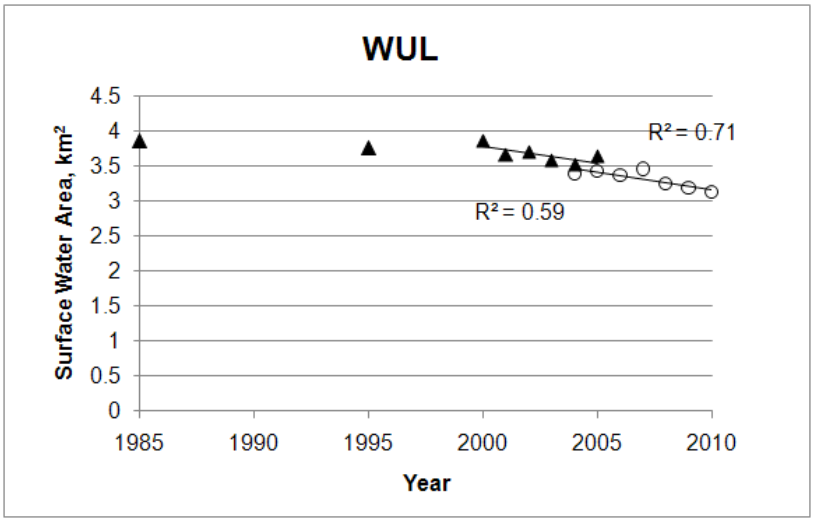

Figure 30. Plot of total surface water area vs. year for the Wulik Lowland subsection.

Figure 31. Lakes in the Wulik Lowland subsection. The large lake in the middle of this July 2001 photograph (NHD #41761330 in the Appendix) was in the process of draining by a channel through the far bank. By 2003 it had less than half of its pre-2000 surface area.

Gates of the Arctic National Park and Preserve

Most of the lakes in the GAAR valleys occupy basins in glacial deposits, with minor thermokarst modification. Recall that the lake analysis areas in these valleys were drawn to exclude river floodplains and associated flooding-influenced lakes.

All of the GAAR study areas showed statistically significant lake area declines in the period 2004-2010. Rates of decline were greatest in the Kobuk and Koyukuk River Valley lake areas, -1.41%/year and -2.85%/year, respectively, and final lake areas there were well below what was present in the 1980s and 1990s.

Alatna River Valley (Alatna)

Lake area fluctuated irregularly prior to 2006 before declining at a statistically significant rate, though with a rather gentle slope (-0.6%/year), to a level about 5% below was it was 1985-2000.

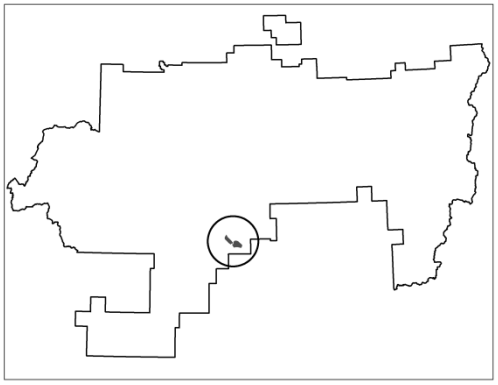

Figure 32. Location of the Alatna River Valley lake area in GAAR

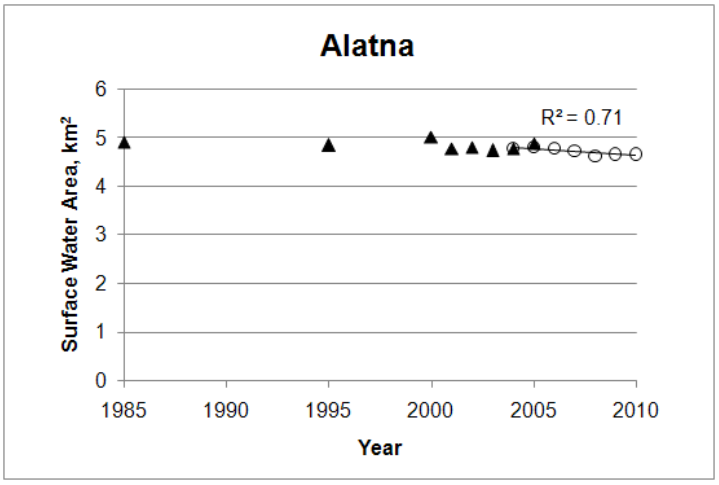

Figure 33. Plot of total surface water area vs. year for the Alatna River Valley lake area.

Itkillik River Valley (Itkillik)

The trend in the Itkillik River Valley was similar to the Alatna Valley, with an even more gentle decline (-0.2%/year) and the final area was within a few percent of what it was 1985-2000.

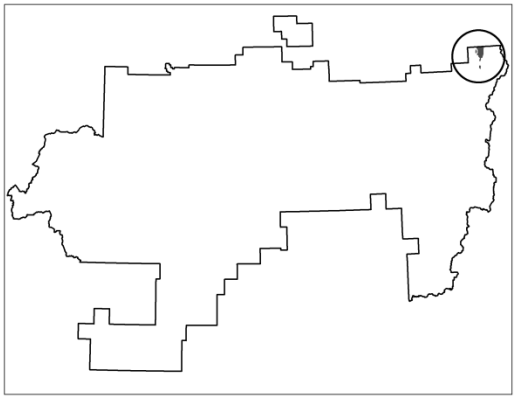

Figure 34. Location of the Itkillik River Valley lake area in GAAR

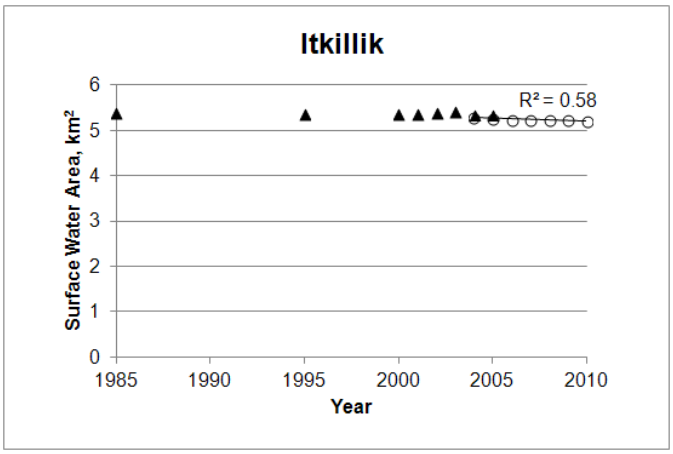

Figure 35. Plot of total surface water area vs. year for the Itkillik River Valley lake area.

Killik River Valley (Killik)

The trend here was very similar to the Alatna Valley, with a statistically significant decline after 2004, a rather gentle slope of -0.6%/year, and final area about 5% below the 1985-2000 values.

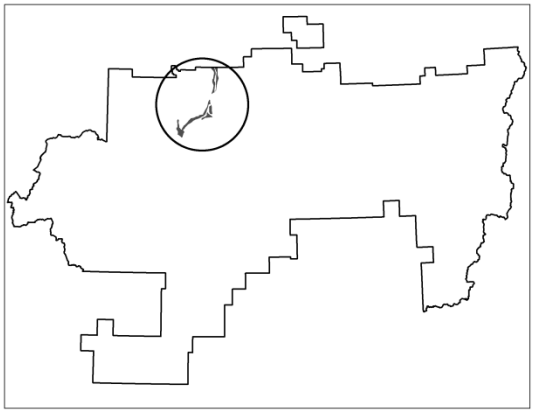

Figure 36. Location of the Killik River Valley lake area in GAAR

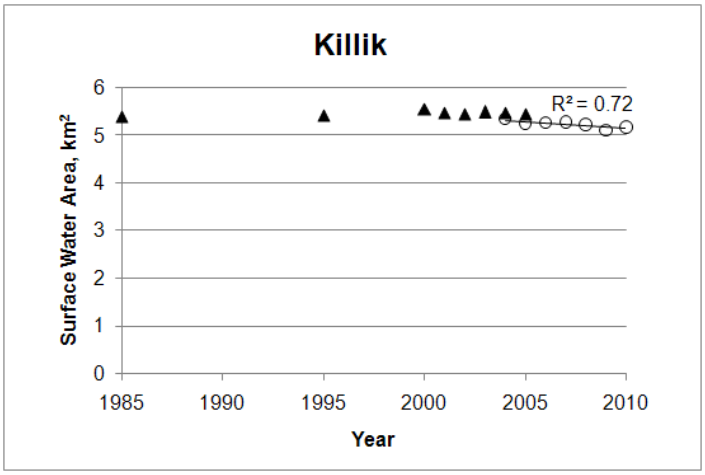

Figure 37. Plot of total surface water area vs. year for the Killik River Valley lake area.

Kobuk River Valley (Kobuk)

The Kobuk River Valley lake study area combines more diverse landscapes than the others, as it includes all of the lake-rich terrain in the Kobuk Preserve Unit. Part of the apparent decline from 2000 to 2005 is driven by erroneously high values for 2000 and 2001 due to clouds, and without these two years the remaining 4 years do not have a significant regression. Nonetheless the area in 2003-2005 appears to be about 17% below 1985 and 9% below the 1990s. Lake area continued to decline fairly rapidly (-1.41%/year) during 2004-2010, due to the shrinkage of multiple small ponds. By the end of the 2000 decade lake, area was well below levels in the 1980s and 1990s.

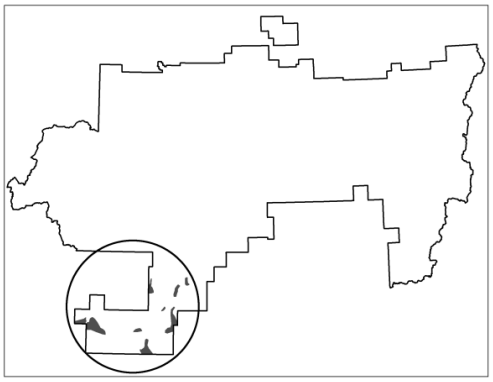

Figure 38. Location of the Kobuk River Valley lake area in GAAR

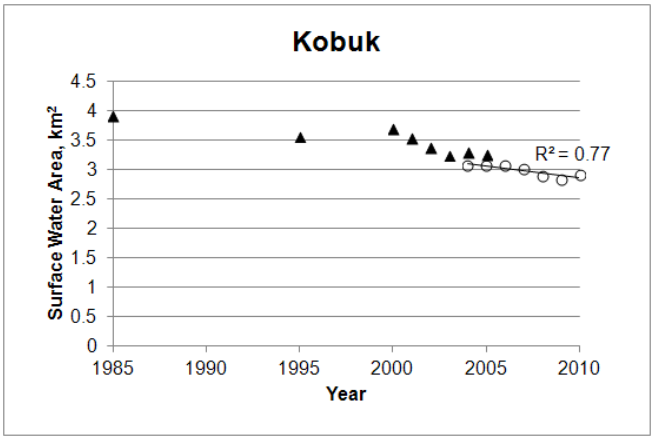

Figure 39. Plot of total surface water area vs. year for the Kobuk River Valley lake area.

Koyukuk River Valley (Koyukuk)

The anomalously high value in 2004 is due to a cloud error and was omitted from the analysis. The remaining 5 points from 2000-2005 show a statistically significant decline in lake area, and moderate slope of -0.9%/year. Like the other GAAR river valleys, there was also a significant decline 2004-2010; in the Koyukuk Valley the rate of decline was more rapid, averaging -2.85%/year since 2004. This decline occurred by shrinkage of multiple lakes. By the end of the 2000 decade lake area was about 20% below what it was in the 1980s and 1990s.

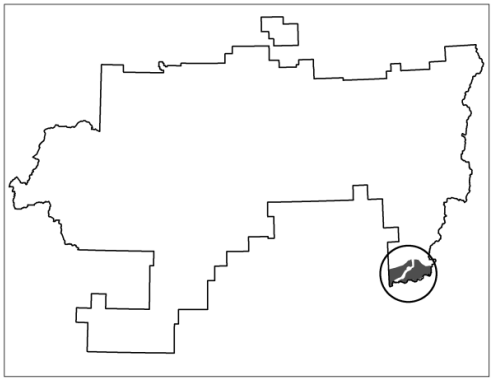

Figure 40. Location of the Koyukuk River Valley lake area in GAAR

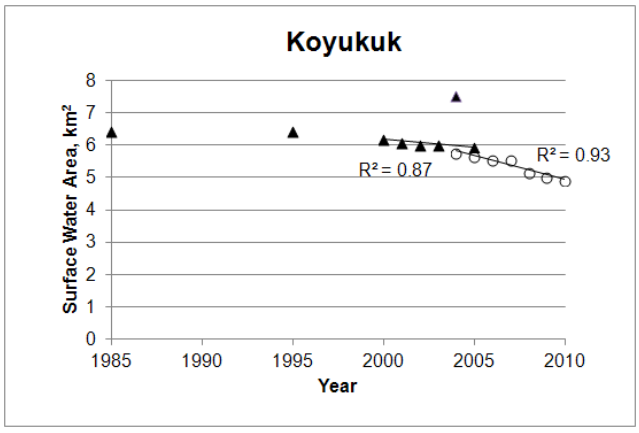

Figure 41. Plot of total surface water area vs. year for the Koyukuk River Valley lake area.

Nigu River Valley (Nigu)

The trend here is similar to the other northern GAAR valleys, with a significant decline 2004-2010. The apparent small upturn in 2010 is actually due to a cloud error, and this year was omitted from the analysis. The slope for 2004-2010 was moderate, -0.89%/year. Lake basins are primarily in glacial depressions with little modification by thermokarst (Fig. 44)

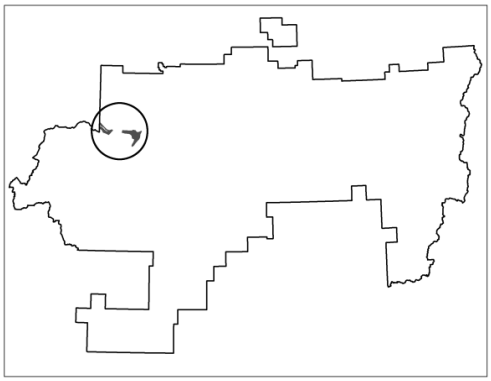

Figure 42. Location of the Nigu River Valley lake area in GAAR

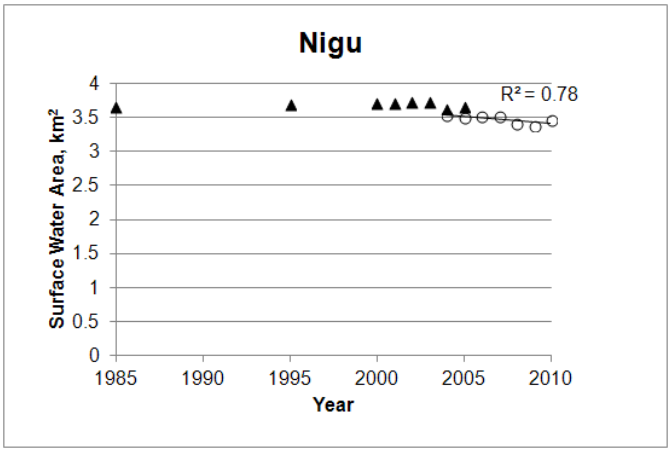

Figure 43. Plot of total surface water area vs. year for the Nigu River Valley lake area.

Figure 44. Lakes in the Nigu River Valley analysis area of GAAR. Like most lakes in the mountain valleys of GAAR, these lakes occupy basins in glacial deposits, with little modification by thermokarst.

Noatak River Valley (Noatak)

Similar to other northern and central GAAR valleys, there was a significant negative trend in lake area since 2004, with a modest slope (-0.6%/year). Lake basins are primarily in glacial depressions with little modification by thermokarst.

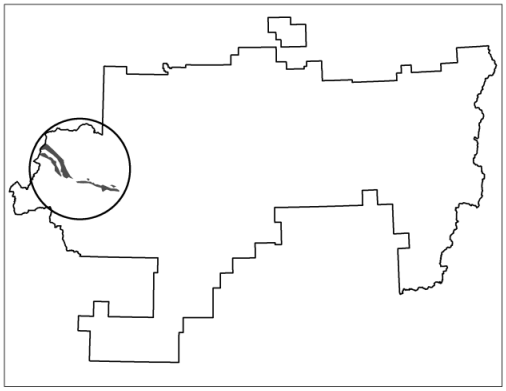

Figure 44. Location of the Noatak River Valley lake area in GAAR

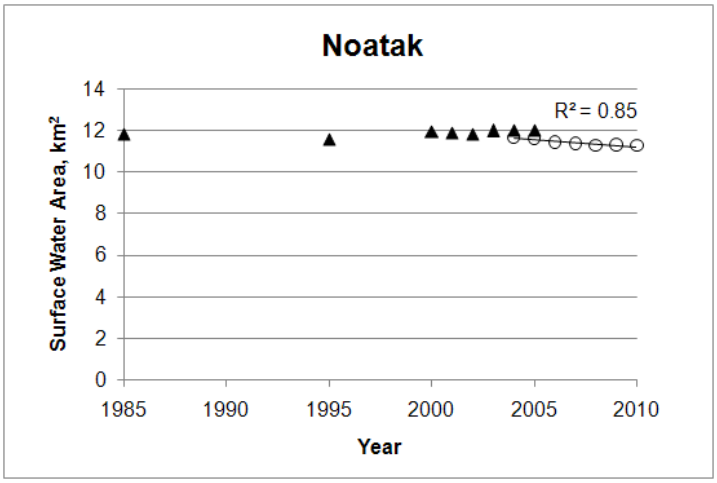

Figure 45. Plot of total surface water area vs. year for the Noatak River Valley lake area.

Kobuk Valley National Park

The three lake-rich subsections in KOVA had different lake-change stories. One (AHW) showed little change, while another (AKP) varied significantly, though change was mainly driven by fluctuations in one large lake. The most important trend was in the third subsection (NIP), where lake area was fairly stable until the middle of the 2000s, when it began a quite precipitous decline due to erosion of outlets into multiple lakes.

Ahnewetut Wetlands (AHW)

The numerous lakes in this subsection occur in depressions on a sand plain near the Great Kobuk Sand Dunes. Lake area appears to have been slightly higher in 1995 and the early 2000s than either today or 1985, though neither regression slope (2000-2005 or 2004-2010) was significant. Ice-wedge polygons are common between the lakes. Informal observations of aerial photographs show that in some areas of the Ahnewetut Wetlands, the ice-wedge polygons have changed from flat or low-centered in the 1950s to high-centered today, which indicates that ice wedges have degraded (Fig. 50). It is interesting that this wedge degradation has not led to lake drainage, probably because the lakes occupy non-thermokarst depressions in the sand sheet.

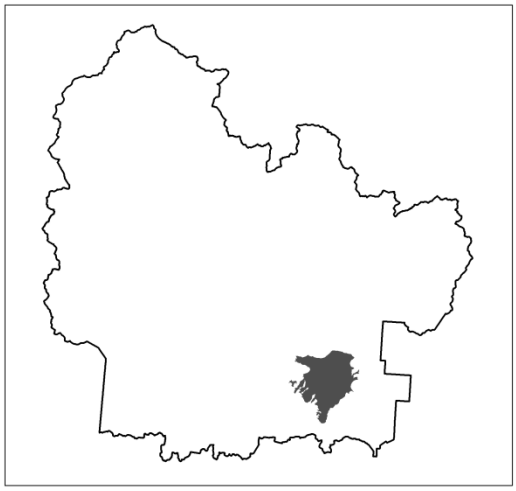

Figure 47. Location of the Ahnewetut Wetlands subsection in KOVA

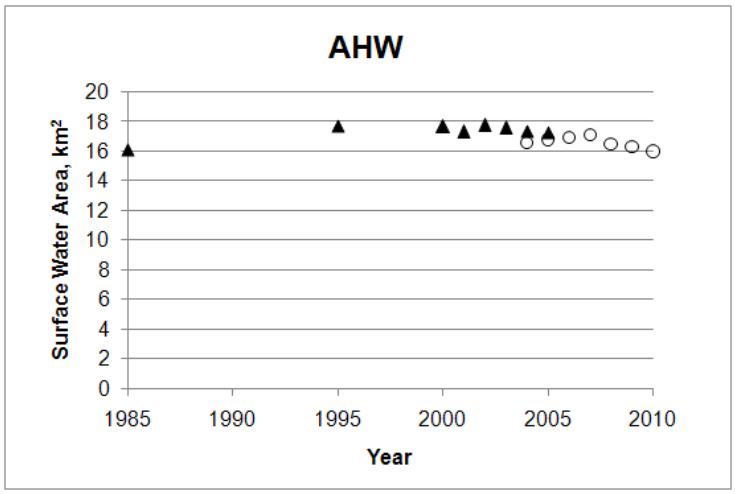

Figure 48. Plot of total surface water area vs. year for the Ahnewetut Wetlands subsection.

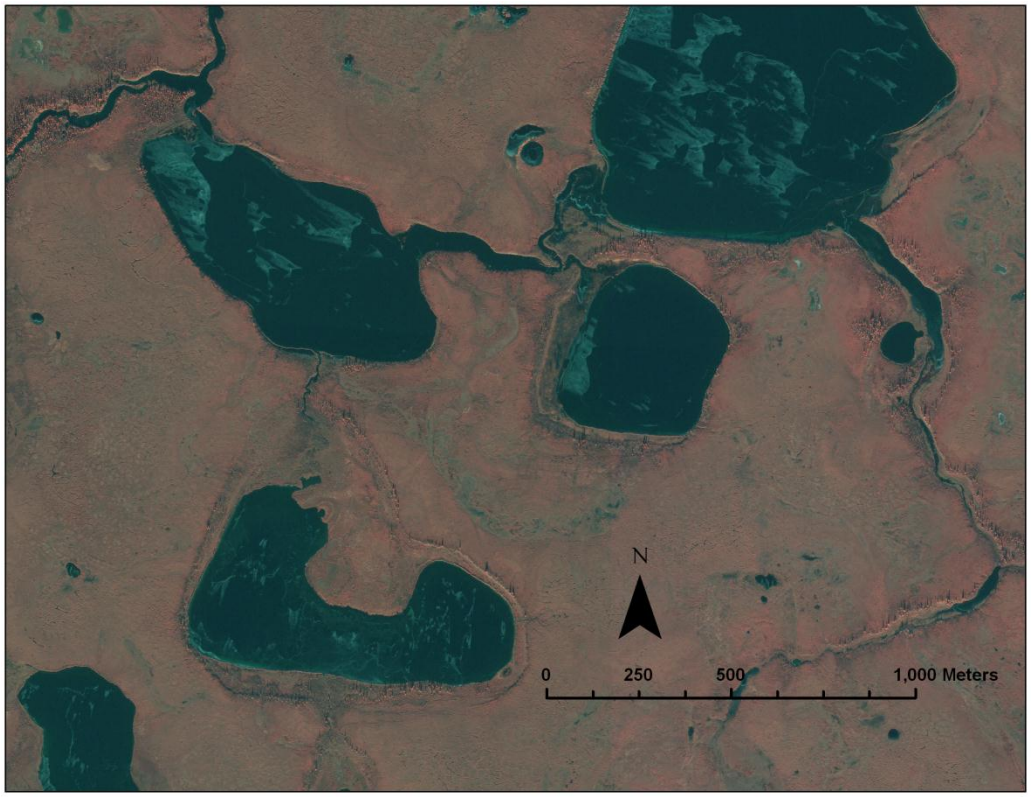

Figure 49. Landscape of the Ahnewetut Wetlands subsection. Numerous sand-bottomed lakes occupy shallow depressions in a sand plain near the Great Kobuk Sand Dunes. Rivers have breached some of the lakes in this area, but, as a result of high water levels in the rivers, the lakes persist.

Figure 50. Degraded ice wedges in the Ahnewetut Wetlands. Melt of ice wedges has caused subsidence along ice-wedge polygon boundaries, which are now marked by water-filled troughs. This process has not led to drainage of lakes such as the one just visible along the skyline on the right-center of the photo, because the lakes occupy basins lower than the polygon surface.

Akillik Plain (AKP)

Most of the lakes on the Akillik Plain occur on old glacial deposits on the eastern part of the subsection, in a lowland area with a largely integrated drainage network. Lake area declined by about 1 km^2 (14%) from 1985 to 1995, due to the drainage of several lakes, but primarily one large lake about 1 km^2 in size (Fig. 53, Appendix). This large lake had refilled by 2005, apparently due to beaver dams on its outlet (Fig. 53), and then shrank again a few years later. This subsection is unique in showing both a significant increase in lake area 2000-2005 (though never attaining the 1985 level) and a significant decrease 2004-2010, both controlled mainly by the fluctuations of this single large lake.

Figure 51. Location of the Akillik Plain subsection in KOVA

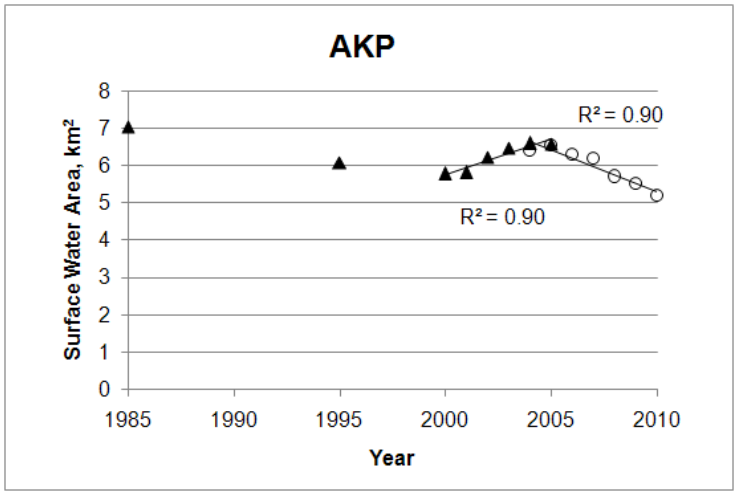

Figure 52. Plot of total surface water area vs. year for the Akillik Plain subsection.

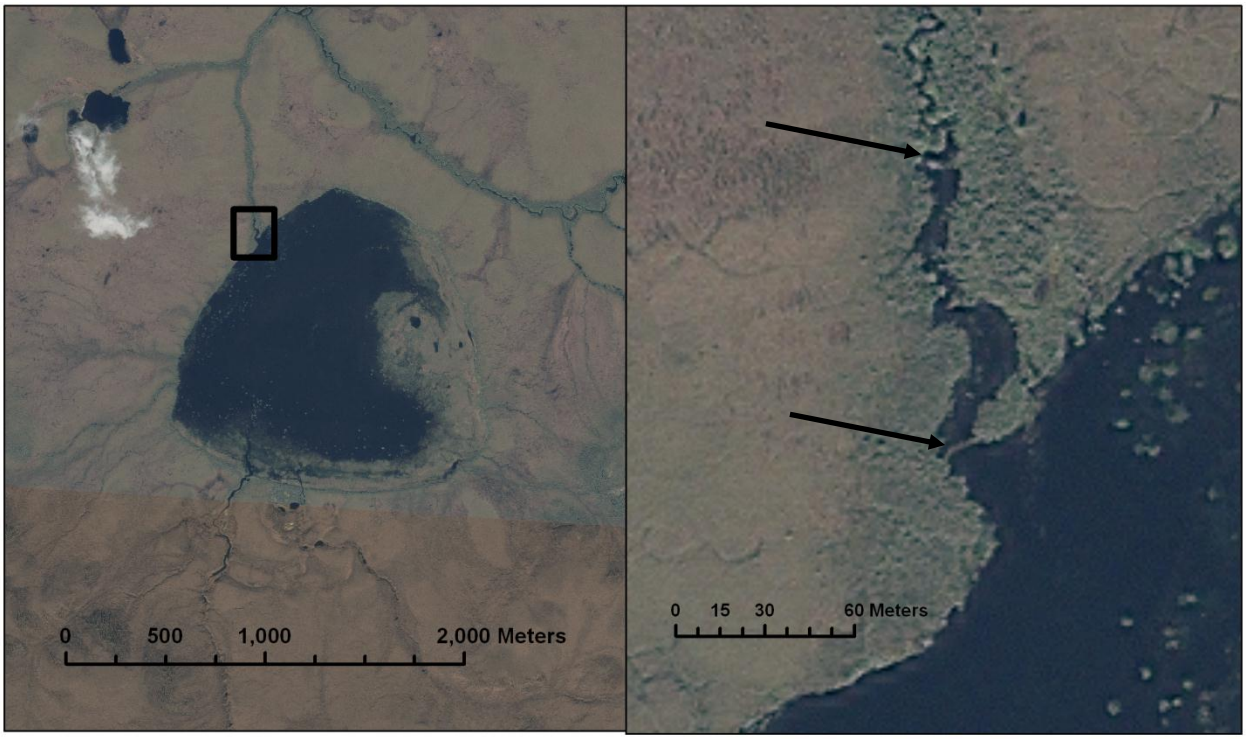

Figure 53. Fluctuations in this lake (NHD #32431047) have largely determined the water surface area in the Akillik Plain subsection. On the left is a 2008 natural color IKONOS image of the whole lake. The image on the right is an enlargement of the outlet area, shown by the black box on the left image. In 1985 the lake was full to about the extent shown, but by 1992 it had shrunk to less than one quarter of this size. Then it filled again to an even higher level in 2005 before gradually declining again. A likely explanation for these fluctuations is beaver dams, which are noted with arrows on the magnified image of the outlet area (right).

Nigeruk Plain (NIP)

The Nigeruk Plain is an area of ice-rich windblown sediments with numerous small thermokarst lakes. Portions of the Nigeruk Plain probably have Pleistocene ice masses similar to the yedoma of BELA, though not as ice-rich as shown by the shallower lake basins. Lake area fluctuated without obvious trend until 2005, when it started to drop, with an especially steep decline 2007-2009. The regression slope here was significant and more than -3%/year for the period 2004-2010. By 2010 the lake area was about 20% below what it was in the 1980s and 1990s. Many lakes drained during the study period (Appendix), and many others showed shrinkage of some kind. Most lakes drained by breaching of the bank and erosion of an outlet (Fig. 56).

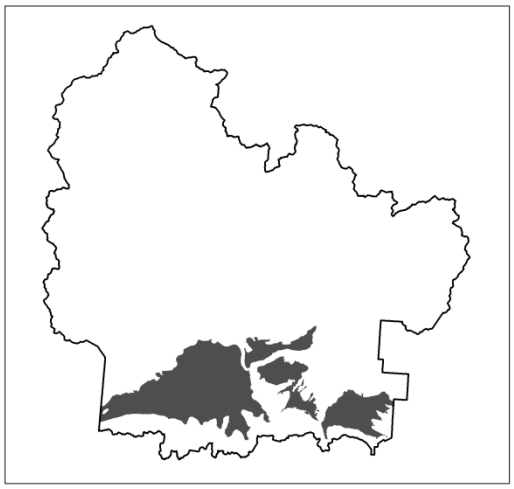

Figure 54. Location of the Nigeruk Plain subsection in KOVA

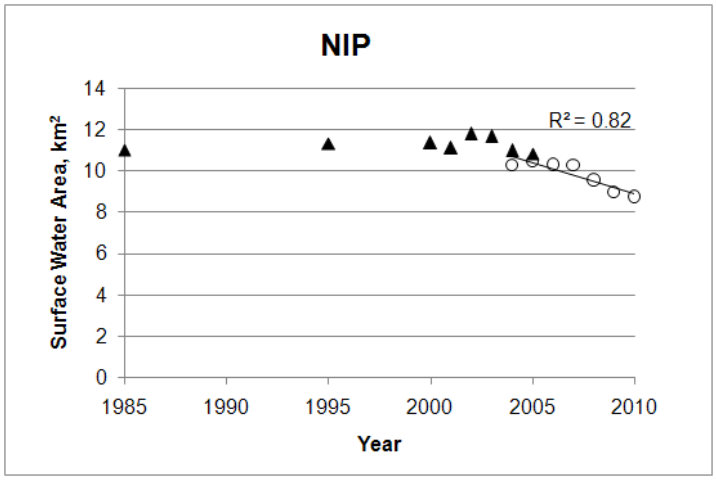

Figure 55. Plot of total surface water area vs. year for the Nigeruk Plain subsection.

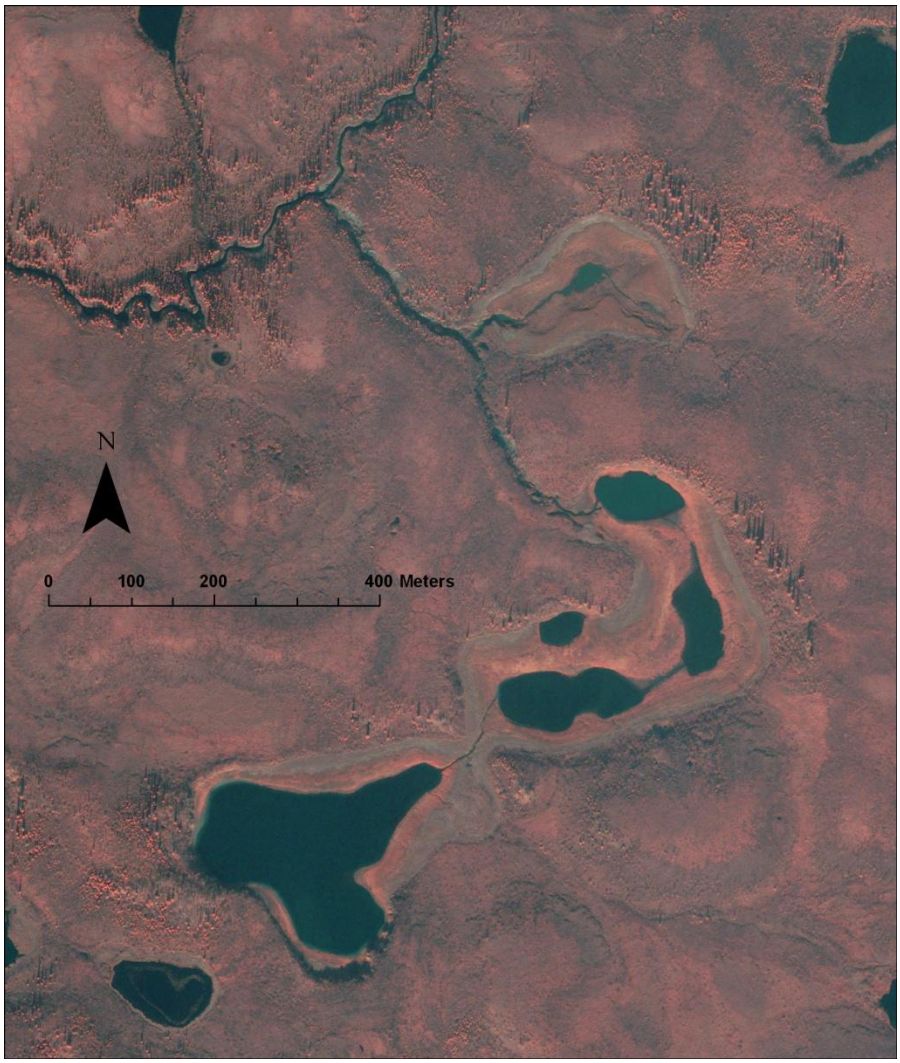

Figure 56. Three lake basins on the Nigeruk Plain that have drained to varying degrees by formation of an outlet to a nearby creek. Between 2003 and 2004 a new channel eroded and drained the northernmost of the 3 basins (NHD #32436690) almost completely while the middle and southern lakes only partly drained. Lake levels then stabilized near the point shown in this September 2006 IKONOS satellite image (color-infrared color scheme) and persisted with little change through 2010.

Noatak National Preserve

All of the study subsections in NOAT consist of glacial deposits with lakes in non-thermokarst depressions, except for the Lower Noatak Lowlands, which is a typical thermokarst lake plain. The latter subsection showed weak trends after a major lake drainage event just prior to the beginning of our study period in 1985. All of the glacial subsections showed significant declines in lake area for the 2004-2010 time period ($P < 0.05$ for all regressions). However, the amount of decline varied: in some it was rather small (e.g., a change of just -0.4%/year and final lake area similar to what was present in the 1980s and 1990s, in subsections AGU and MNU); in other subsections the rate of decline in 2004-2010 was greater than -1%/year and final lake areas were 10% or more below what was present in the 1980s and 1990s (subsections NGL and UNB). Other subsections showed changes intermediate between these two extremes.

Avingyak Glaciated Uplands (AGU)

This subsection is dominated by two large lakes, Desperation and Feniak. Lake area was very stable from 1985-2005. A drop in lake area after 2005 was statistically significant, but the rate of change was quite slow (-0.4%/year).

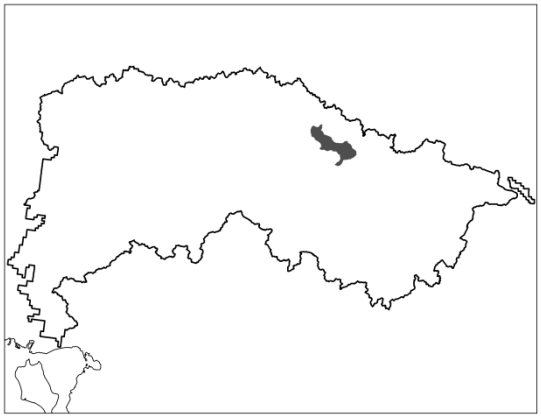

Figure 57. Location of the Avingyak Glaciated Uplands subsection in NOAT

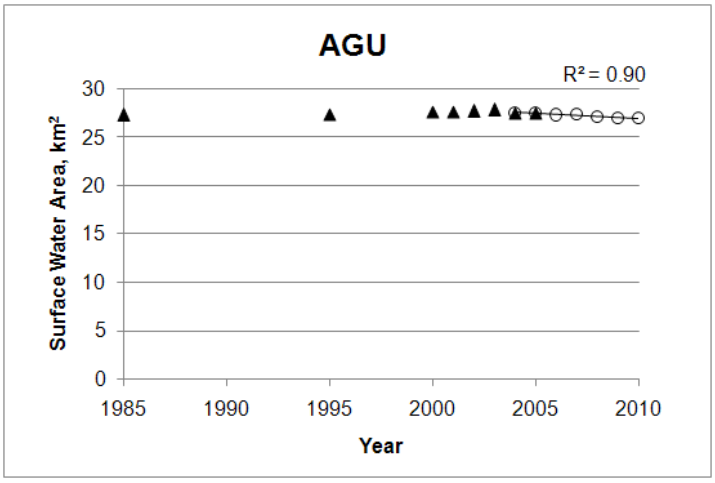

Figure 58. Plot of total surface water area vs. year for the Avingyak Glaciated Uplands subsection.

Iggiruk Uplands (IGU)

This is another subsection with largely stable lake basins in glacial deposits. Changes were generally minor, though there was a significant downward trend 2004-2010 (through shrinkage of many lakes). The 2010 area was only slightly below the 1985 value.

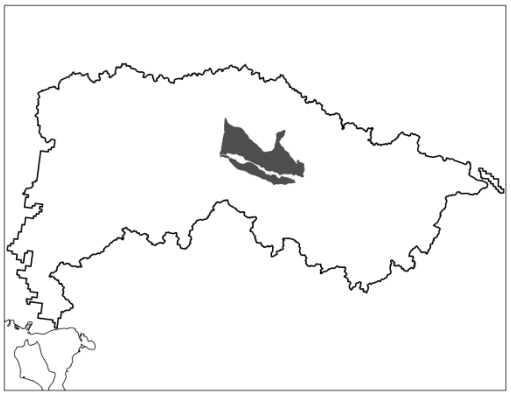

Figure 59. Location of the Iggiruk Uplands subsection in NOAT

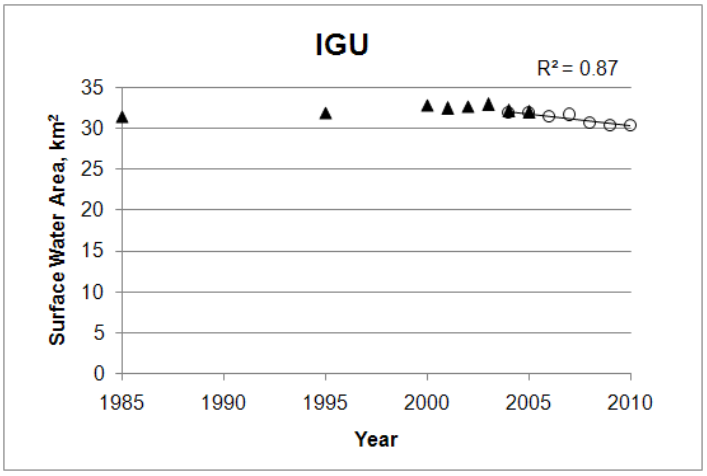

Figure 60. Plot of total surface water area vs. year for the Iggiruk Uplands subsection.

Kavachurak Glaciated Uplands (KGU)

This moraine lake area showed more substantial declines than the preceding subsections in NOAT, with significant regressions for both time periods and steeper downward slopes (-1.15 and -0.76%/year). Water area declined about 10% during the 2000 decade.

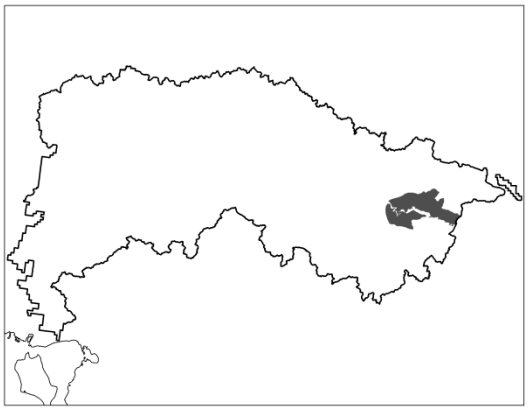

Figure 61. Location of the Kavachurak Glaciated Uplands subsection in NOAT

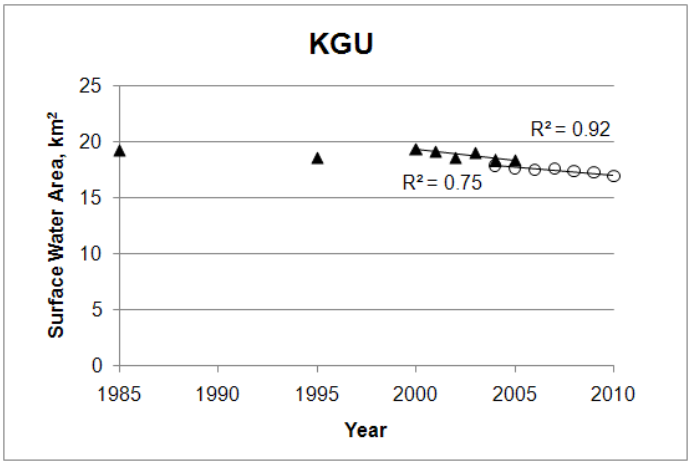

Figure 62. Plot of total surface water area vs. year for the Kavachurak Glaciated Uplands subsection.

Lower Noatak Lowlands (LNL)

This subsection is an extensive plain of overlapping thaw lake basins. The total lake area fluctuated without any clear trend. Two small lake drainage events occurred between 1985 and 1992 (Appendix). A more significant drainage event occurred just prior to our first image year (1985; Fig. 65).

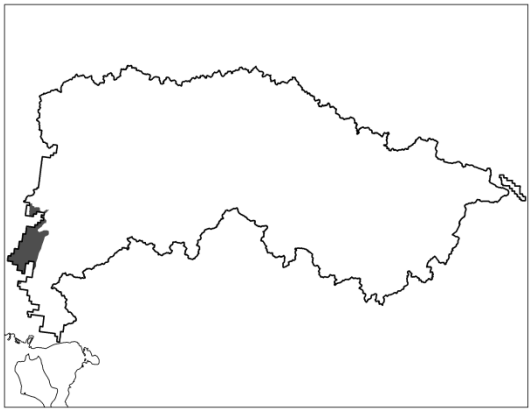

Figure 63. Location of the Lower Noatak Lowlands subsection in NOAT

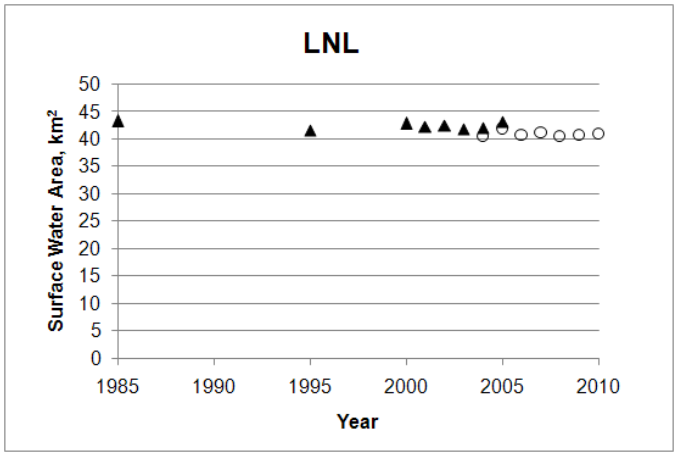

Figure 64. Plot of total surface water area vs. year for the Lower Noatak Lowlands subsection.

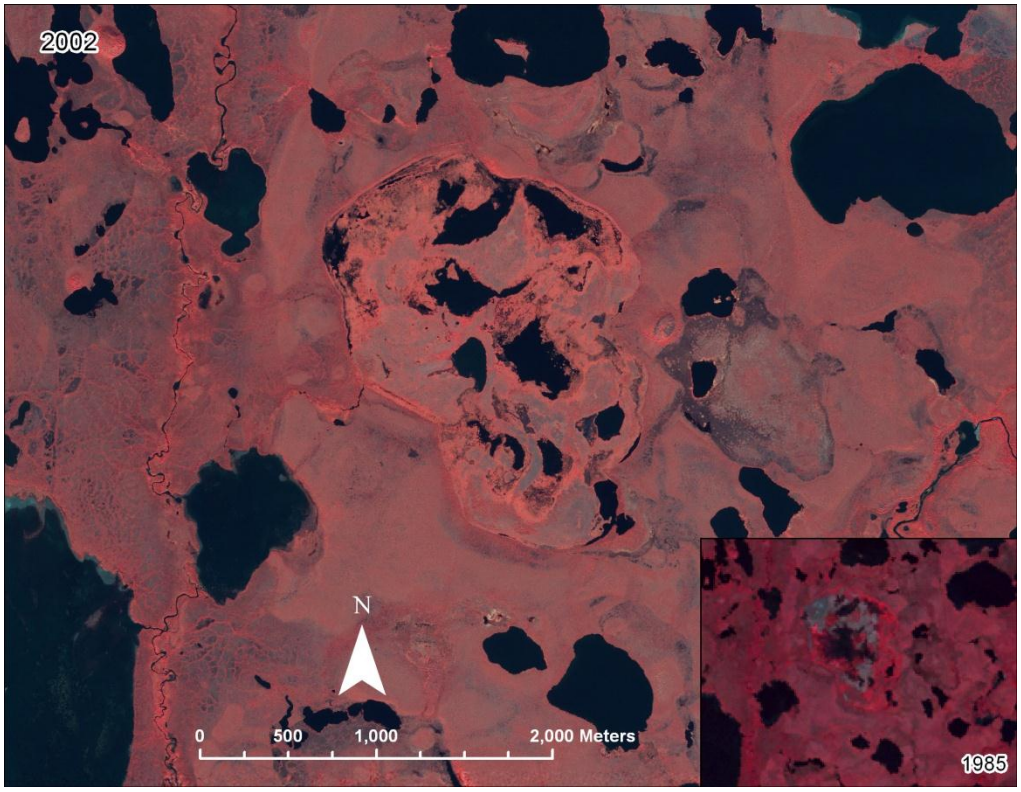

Figure 65. Lower Noatak Lowlands subsection, IKONOS image 2002 (inset map, Landsat image, 1985), color-infrared color scheme. This subsection has many overlapping lake basins of thermokarst origin, some still occupied by lakes and others drained for various lengths of time. The large partly drained basin in the center of this figure drained just prior to 1985, as shown by the gray, unvegetated areas in 1985.

Middle Noatak Uplands (MNU)

Minor fluctuations in lake area in this subsection with glacial deposits were followed by a downward trend that was significant but not very steep (slope -0.4%/year).

Figure 66. Location of the Middle Noatak Uplands subsection in NOAT

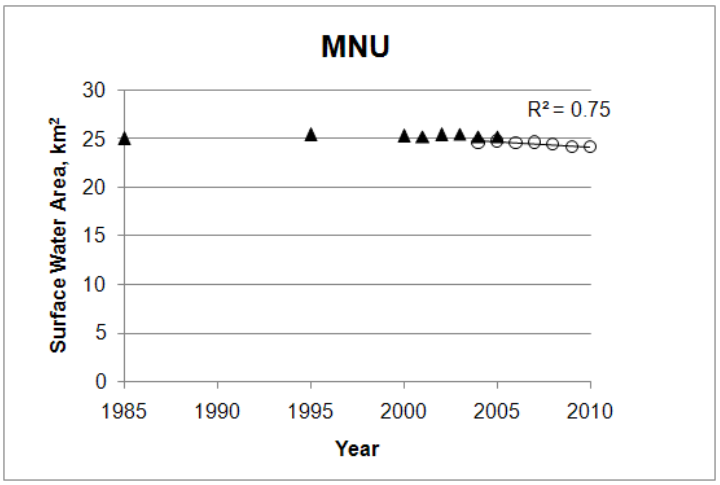

Figure 67. Plot of total surface water area vs. year for the Middle Noatak Uplands subsection.

Noatak Glaciated Lowlands (NGL)

This subsection showed a strong downward trend after 2000. Both the 2000-2005 and 2004-2010 time periods showed significant regression slopes steeper than -1%/year. Lake area loss was by shrinkage of many lakes (rather than complete drainage of a few), and final areas were about 13% below the areas in the 1980s and1990s.

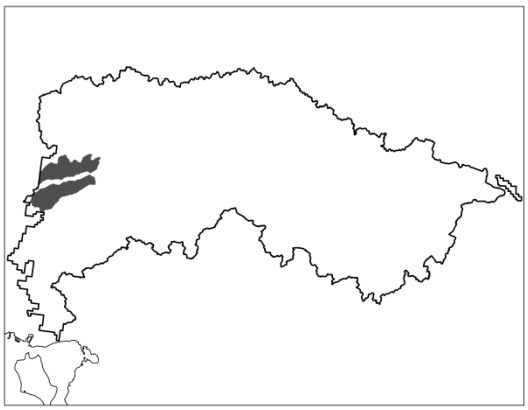

Figure 68. Location of the Noatak Glaciated Lowlands subsection in NOAT

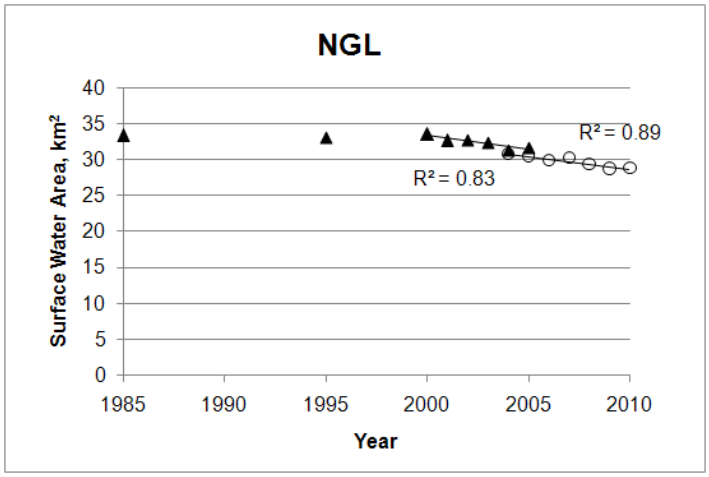

Figure 69. Plot of total surface water area vs. year for the Noatak Glaciated Lowlands subsection.

Nigu Mountain Valley (NGU)

Here the downward trend was significant but only brought the level back to about what it was in 1985. This subsection includes a river floodplain, which adds some error to water surface area measurement.

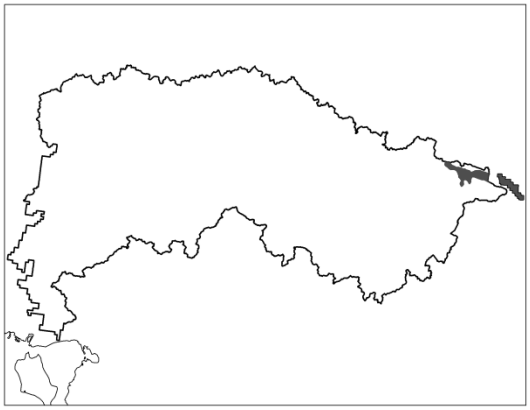

Figure 70. Location of the Nigu Mountain Valley subsection in NOAT

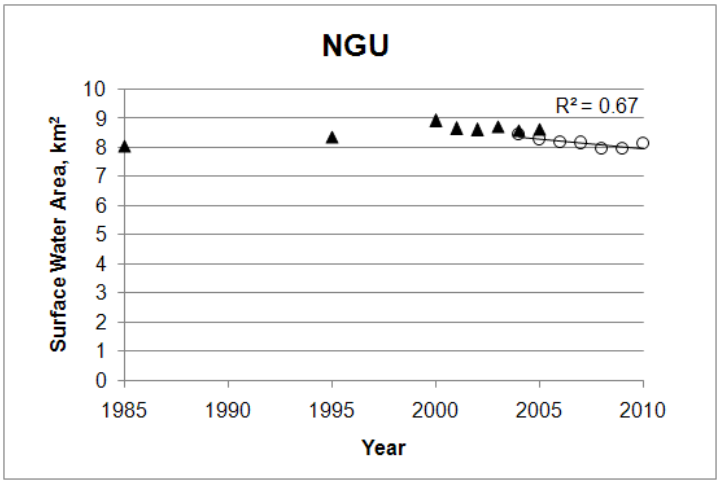

Figure 71. Plot of total surface water area vs. year for the Nigu Mountain Valley subsection.

Upper Noatak Basin (UNB)

Lake area appears to have increased from 1985 to 2000, though there is some uncertainty with just 3 data points. Lake area then declined steadily after 2000: the regressions for both the 2000-2005 and 2004-2010 time periods were significantly negative, and the 2004-2010 regression had a quite steep slope (-1.6%/year). Water area declined about 14% during the 2000 decade, but final areas were only about 7% below what they were in 1985. The decline was by minor shrinkage of many lakes.

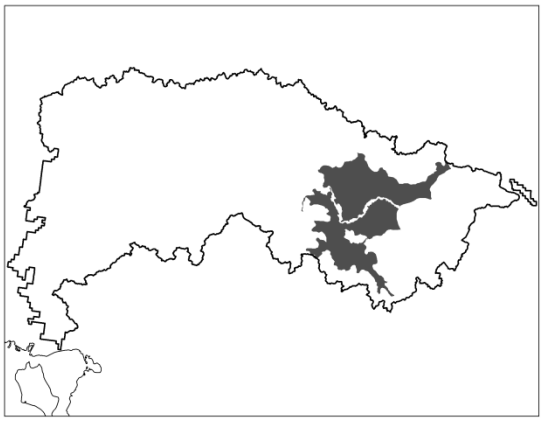

Figure 72. Location of the Upper Noatak Basin subsection in NOAT

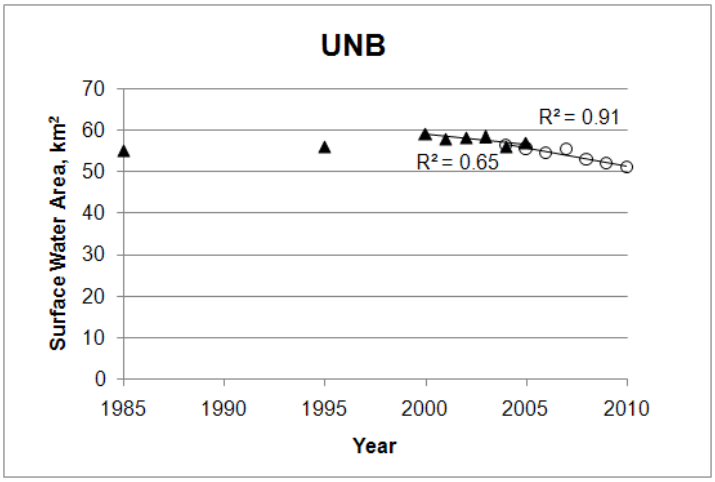

Figure 73. Plot of total surface water area vs. year for the Upper Noatak Basin subsection.

Discussion

Declines in lake area in permafrost regions of Alaska have been attributed to drainage by erosion of outlets in a permafrost basin, by loss of water by percolation through newly thawed permafrost under water bodies, by a shift in the balance between precipitation and evapotranspiration in the lake's watershed, and by terrestrialization (encroachment of vegetation and infilling with organic matter) (Yoshikawa and Hinzman 2003, Riordan et al. 2006, Jones et al. 2011, Roach et al. 2011). All of these mechanisms have probably been at work in various parts of ARCN. As mentioned previously, lakes on floodplains, which could additionally be influenced by river flood frequency and duration, were excluded from this study.

Lake drainage by erosion of new or deeper outlets has been active in the subsections with thermokarst lakes such as the Nigeruk Plain in KOVA and the Bering Straits Lower Coastal Plain in BELA (Jones et al. 2011, for the latter area). Lake drainage events by erosion of a new outlet are also not uncommon on old glacial deposits such as the Lower Noatak Moraine in CAKR and Akillik Plain in KOVA, where lakes have a combined glacial and thermokarst origin. We suspect that lake drainage events have been more frequent in the last decade in these areas because permafrost degradation (Jorgenson 2006) has enhanced the formation of drainage outlets. These outlets could develop by thermokarst expansion of the lake basin into a lower-lying area or formation of drainage channels along melting ice wedge networks (Jones et al. 2011; Fig. 74).

Figure 74. Oblique aerial photograph of ice wedges melting to form channels. The area shown is about 50 m wide and the channels are about 2 m deep. The ice from fall freeze-up is visible around the small ponds. Noatak National Preserve, Sept 2012, -157.5345° longitude, 67.8230° latitude.

However, major lake drainage events do not account for all of the lake area loss, even in the thermokarst lake areas. For example, in the Nigeruk Plain over 1.5 km^2 of lake area was lost in the 2000 decade (Fig. 55), while we have identified only about 0.6 km^2 of lake drainage events (Appendix). Similarly, in the 2000s we identified about 10 km of lake drainage events in the Bering Straits Lower Coastal Plain (Appendix), while the total area lost during this time was about 14 km^2. Thus one or more of the other mechanisms mentioned above must also be acting, even in these dominantly thermokarst lake areas.

Lake drainage events in younger moraines with little thermokarst activity (i.e. deposits of the Itkillik glaciations: Hamilton 2010, Hamilton and Labay 2011) were very rare: we identified just one such event, which occurred in a lake very near to an incised river (Fig. 75). This lake was in the Kaluktavik Uplands of NOAT (KLU, see the Appendix), a subsection with too few lakes to be included in our lake-area analysis. Loss of lake area in the regions of stable, non-thermokarst lake basins on glacial deposits must be by loss of permafrost under the lake, change in the balance between precipitation and evapotranspiration, or terrestrialization.

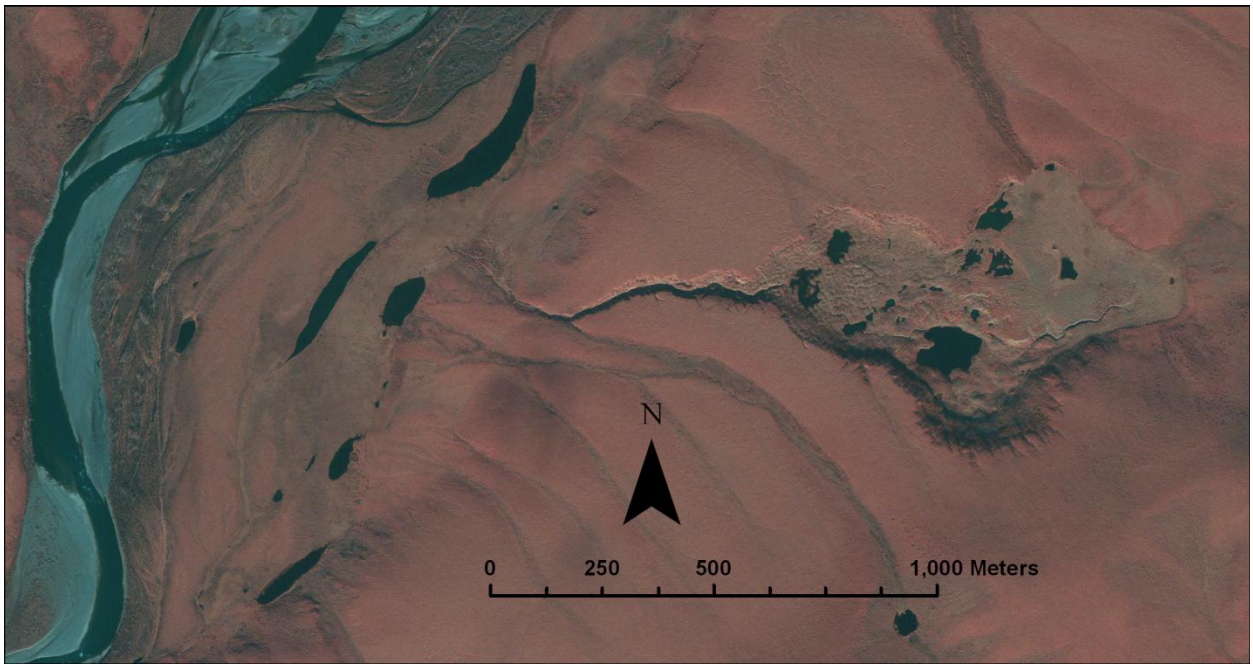

Figure 75. Drainage of a non-thermokarst lake on a late Pleistocene moraine in NOAT. An outlet eroded to the Kugururok River Valley between 1985 and 1992. Angular traces of ice wedges along the channel (especially the south side near the lake basin) suggest that ice wedge melt enhance the formation of this channel. Drainage of lakes is rare on these relatively ice-poor moraines. Oct 2006 color-IR IKONOS image, -161.48° longitude, 68.12° latitude

The climatic drivers of the observed changes of lake areas in ARCN are not clear. Warming climate, leading to permafrost degradation and thermokarst, could cause both lake basin expansion and erosion of new drainage outlets. The water balance could change through increased evapotranspiration (from longer or warmer summers) or less precipitation. Analysis of temperature trends in Alaska over recent decades indicate an abrupt change to warmer temperatures in the mid 1970s followed by slight cooling since 2000 (Hartman and Wendler 2005, Wendler et al. 2012). Cursory examination of the temperature data from National Weather

Service (NWS) stations near ARCN (Bettles and Kotzebue; WRCC 2012; Fig. 1) and Remote Alaska Weather Stations (RAWS, WRCC 2011) in ARCN suggest that park climates have followed the statewide trends. It is possible that ongoing permafrost thaw in response to the 1970s warming event caused increased rates of lake drainage in the 2000s. Precipitation records are available only at Kotzebue and Bettles (the RAWS record only temperature year-round), and precipitation records from Kotzebue are suspect because NWS rain gages in windy places like Kotebue have difficulty capturing snow (Clagett 1988). Nonetheless, an estimate of the lake water balance for Kotzebue (annual precipitation minus evapotranspiration) by Jones et al. (2011) shows a decline from the mid 1990s to late 2000s that, if widespread, could be responsible for some of the observed lake-area decline in non-thermokarst subsections.

Literature Cited

Billings, W. D. and K. M. Peterson. 1980. Vegetational change and ice-wedge polygons through the thaw-lake cycle in arctic Alaska. Arctic and Alpine Research 12(4):413-432.

Beget, J. E., D. M. Hopkins, and S. D. Charron. 1996. The largest known maars on earth, Seward Peninsula, northwest Alaska. Arctic 49(1):62-69.

Boggs, K., and J. Michaelson. 2001. Ecological subsections of Gates of the Arctic National Park and Preserve. Inventory and Monitoring Program, National Park Service, Alaska Region, Anchorage, Alaska.

Clagett G. P. 1988. The Wyoming windshield: an evaluation after 12 years of use in Alaska. Proceedings of the Western Snow Conference, April 1988, Kalispell, Montana. Available from http://www.westernsnowconference.org/proceedings/pdf_Proceedings/1988%20WEB/Claget t,TheWyomingWindshieldAlaska.pdf (accessed 21 December 2012).

Czudek, T. and J. Demek. 1970. Thermokarst in Siberia and its influence on the development of lowland relief. Quaternary Research 1:103–120.

Hamilton, T. D. 2010. Surficial geologic map of the Noatak National Preserve, Alaska. Scientific Investigations Map 3036. U.S. Geological Survey, Federal Center, Colorado, scale 1:250,000.

Hamilton, T. D. and K. A. Labay. 2011. Surficial geologic map of the Gates of the Arctic National Park and Preserve, Alaska. Scientific Investigations Map 3125. U.S. Geological Survey, Federal Center, Colorado, scale 1:250,000.

Hartmann, B., and G. Wendler. 2005. The significance of the 1976 Pacific climate shift in the climatology of Alaska. Journal of Climate 18:4824–4839.

Hopkins, D. M. 1949. Thaw lakes and thaw sinks in the Imuruk Lake area, Seward Peninsula, Alaska. Journal of Geology 57:119-131

Hopkins, D. M. 1963. Geology of the Imuruk Lake area, Seward Peninsula, Alaska. Geological Survey Bulletin 1141-C. U. S. Geological Survey, Washington, D. C.

Jones B. M., G. Grosse, C. D. Arp, M. C. Jones, K. M. Walter Anthony, and V. E. Romanovsky. 2011. Modern thermokarst lake dynamics in the continuous permafrost zone, northern Seward Peninsula, Alaska. Journal of Geophysical Research 116, G00M03, doi:10.1029/2011JG001666.

Jorgenson, M. T. and T. E. Osterkamp. 2005. Response of boreal ecosystems to varying modes of permafrost degradation. Canadian Journal of Forest Research 35:2100-2111.

Jorgenson, M. T., Y. L. Shur, and E. R. Pullman. 2006. Abrupt increase in permafrost degradation in Alaska. Geophysical Research Letters 33:L02503.

Jorgenson, M. T. and Y. Shur. 2007. Evolution of lakes and basins in northern Alaska and discussion of the thaw lake cycle. Journal of Geophysical Research 112, F02S17, doi:10.1029/2006JF000531.

Jorgenson, T., K. Yoshikawa, M. Kanevskiy, Y. Shur, V. Romanovsky, S. Marchenko, G. Grosse, J. Brown, and B. Jones. 2008. Permafrost characteristics of Alaska. Proceedings of the Ninth International Conference on Permafrost. University of Alaska Fairbanks, Institute of Northern Engineering.

Jorgenson, M. T. 2001. Ecological subsections of Bering Land Bridge National Preserve. Inventory and Monitoring Program, National Park Service, Alaska Region, Anchorage, Alaska.

Jorgenson, M. T., D. K. Swanson, and M. Macander. 2001. Landscape-level mapping of ecological units for the Noatak National Preserve, Alaska. Inventory and Monitoring Program, National Park Service, Alaska Region, Anchorage, Alaska.

Kane, D.L., and L.D. Hinzman. 1988. Permafrost hydrology of a small arctic watershed. Proceedings: Fifth International Conference on Permafrost, Trondheim, Norway. pp. 590-595.

Kanevskiy, M., Y. Shur, D. Fortier, M. T. Jorgenson, and E. Stephani. 2011. Cryostratigraphy of late Pleistocene syngenetic permafrost (yedoma) in northern Alaska, Itkillik River exposure. Quaternary Research 75:584-596.

Karlstom, T. N. V and others. 1964. Surficial geology of Alaska. U. S. Geological Survey Miscellaneous Geologic Investigations Map I-357, scale 1:1,584,000.

Macander, M. J. and C. S. Swingley. 2012. Mapping snow persistence for the range of the Western Arctic Caribou Herd, northwest Alaska, using the Landsat archive (1985-2011). Natural Resource Technical Report NPS/ARCN/NRTR—2012/643.National Park Service, Fort Collins, Colorado.

Masek, J. G., E. F. Vermote, N. E. Saleous, R. Wolfe, F. G. Hall, F. Huemmrich, F. Gao, J. Kutler, and T. K. Lim. 2006. A Landsat surface reflectance data set for North America, 1990-2000. IEEE Geoscience and Remote Sensing Letters 3(1):69–72.

NASA 2012. The thematic mapper. National Aeronautics and Space Administration. Available from http://landsat.gsfc.nasa.gov/about/tm.html (accessed 14 December 2012).

Osterkamp, T. E. 2007. Characteristics of the recent warming of permafrost in Alaska. Journal of Geophysical Research 112 F02S02, doi:10.1029/2006JF000578.

Plug L. J. and J. J. West. 2009. Thaw lake expansion in a two-dimensional coupled model of heat transfer, thaw subsidence, and mass movement. Journal of Geophysical Research 114: F01002, doi:10.1029/2006JF000740.

Roach, J., B. Griffith, D. Verbyla, and J. Jones. 2011. Mechanisms influencing changes in lake area in Alaskan boreal forest. Global Change Biology 17: 2567–2583, doi: 10.1111/j.1365-2486.2011.02446.x

Roy, D. J. Ju, I. Kommareddy, M. Hansen, E. Vermote, C. Zhang, and A. Kommareddy. 2001. Algorithm theoretical basis Document, Web enabled Landsat Data (WELD) products. Available from http://globalmonitoring.sdstate.edu/projects/weld/WELD_ATBD.pdf (accessed 14 December 2012).

Riordan, B., D. Verbyla, and A. D. McGuire. 2006. Shrinking ponds in subarctic Alaska based on 1950–2002 remotely sensed images. Journal of Geophysical Research 111, G04002, doi:10.1029/2005JG000150.

Roy, D.P., J. Ju, K. Kline, P.L. Scaramuzza, V. Kovalskyy, M.C. Hansen, T.R. Loveland, E.F. Vermote, C. Zhang. 2010. Web-enabled Landsat Data (WELD): Landsat ETM+ Composited Mosaics of the Conterminous United States, Remote Sensing of Environment, 114: 35-49. Available from http://globalmonitoring.sdstate.edu/projects/weld/ (accessed 14 December 2012).

Shur, Y., M. Z. Kanevskiy, M. T. Jorgenson, D. Fortier, M. Dillon, E. Stephani, and M. Bray, 2009. Yedoma and thermokarst in the northern part of Seward Peninsula, Alaska. American Geophysical Union, Fall Meeting 2009, abstract #C41A-0443

Swanson, D. K. 2001a. Ecological subsections of Cape Krusenstern National Monument. Inventory and Monitoring Program, National Park Service, Alaska Region, Anchorage, Alaska.

Swanson, D. K. 2001b. Ecological subsections of Kobuk Valley National Park. Inventory and Monitoring Program, National Park Service, Alaska Region, Anchorage, Alaska.

USGS NHD. 2012. National hydrography dataset. U.S. Geological Survey. Available from http://nhd.usgs.gov/ (accessed 18 December 2012).

Wendler, G., L. Chen, and B. Moore. 2012. The first decade of the new century: a cooling trend for most of Alaska. The Open Atmospheric Science Journal 6:111-116. Available from http://www.benthamscience.com/open/toascj/articles/V006/111TOASCJ.pdf (accessed 21 December 2012).

West, J. J. and L. J. Plug. 2008. Time-dependent morphology of thaw lakes and taliks in deep and shallow ground ice. Journal of Geophysical Research 113: F01009, doi:10.1029/2006JF000696.

Western Regional Climate Center (WRCC). 2012. Western U.S. Climate Historical Summaries. http://www.wrcc.dri.edu/Climsum.html (accessed 11 December 2012).

Western Regional Climate Center (WRCC). 2011. RAWS USA climate archives. http://www.raws.dri.edu/wraws/akF.html (accessed 12 April 2011).

Yoshikawa, K. and L. D. Hinzman. 2003. Shrinking thermokarst ponds and groundwater dynamics in discontinuous permafrost near council, Alaska. Permafrost and Periglacial Processes 14(2):151-160.

Appendix: Major Lake Drainage and Fill Events, 1985-2010

Table 2. Major lake drainage and fill events in ARCN, 1985-2010

Subsection Code	NHD code[1]	Area[1], km^2	Draining		Filling		Comment
			Last Full	First Empty	Last Empty	First Full	
BELA							
BSLCP	32366067	1.578	1985	1995			
	70263053	1.797	1992	1995			partially refilled in the early 2000s
	32360353	0.104	1995	1999			
	70271135	0.17			2005	2008	
	70254163	2.34	2004	2006			partial
	70263245	0.118	2004	2009			
	32360615	0.945	2005	2006			
	32360609	0.071	2005	2006			
	32360357	3.378	2005	2006			
	32362057	3.166	2005	2010			partial
BSUCP	32271623	0.082			1995	2000	
	70266735	0.06			1995	2000	
	120040540	0.131			1995	2000	
	32367462	0.472	2003	2004			
DU	32369203	0.772	1985	1995			
	32364277	0.39	1985	1995			partial
GBLCP	32360767	0.137	1985	1992			
	32361035	0.303	1985	1992			partial
	32361181	0.14			1995	1999	partial
GBUCP	32363109	0.128	1992	1995			
IL	32251830	0.076	2003	2004			
	32252166	0.133	2006	2007			
	32251261	0.033	2007	2008			
	32251279	0.062	2007	2008			
	32243002	0.239	2005	2010			
	32243004	0.077	2005	2010			
	32243048	0.018	2005	2010			
	32243070	0.135	2005	2010			
KZL	32260713	0.065	1999	2000	2000	2001	partial
	32261067	0.034	1985	1992	1992	1995	
	32254753	0.023	2004	2009			
CAKR							
ACP	41755883	0.024	1995	1999			
	41756547	0.11	2005	2007			
LNM	120040149	0.874	1985	1992			
WUL	41761330	0.674	2000	2003			partial
	41760006	0.19	2008	2009			partial

[1]The NHD codes and areas are from the National Hydrography Dataset (USGS NHD 2012)

Table 2. Major lake drainage and fill events in ARCN, 1985-2010 (continued)

Subsection Code	NHD code[1]	Area[1], km^2	Draining		Filling		Comment
			Last Full	First Empty	Last Empty	First Full	
KOVA							
AKP	32434779	0.04	1985	1992			
	32438342	0.036	1985	1992			partial
	32431047	1.1	1985	1992	2001	2004	Partial drainage, then refilled after beaver dam, then dropped again after 2005
	32432793	0.03	2005	2010			
NIP	120033369	0.073	1985	1992			
	32464524	0.276	1985	1992			
	32433170	0.342	2002	2007			
	32433051	0.025	2007	2008			
	32439152	0.041	2006	2007			
	32439885	0.045	2008	2009			
	32439991	0.007	2004	2007			
	32439447	0.036	2004	2010			
	32439749	0.022	2008	2009			
	32436690	0.026	2003	2004			
	32436692	0.064	2003	2004			
NOAT							
KLU	32559439	0.259	1985	1992			
LNL	72935493	0.367	1992	1995			
	72944264	0.143	1985	1992			

[1]The NHD codes and areas are from the National Hydrography Dataset (USGS NHD 2012)